Rate constants for cyclization reactions of α,δ-hydroperoxyalkyl radicals (reaction 10) obtained in this study cannot be compared to other results since no information has been reported for either the gas or the liquid phase. However, relevant literature data are available for cyclization reactions of α,γ-hydroperoxyalkyl radicals in the gas phase. Using the data of Bastow and Cullis[18] at 250–315 °C and Knox and Kinnear[19] at 250–400 °C for the ratio of rates of formation of 2,4-dimethyloxetane to acetone in the combustion of *n*-pentane gives $k_{10\text{-}\alpha,\gamma} = 10^{12}\exp(-17.5/RT)\ s^{-1}$. From this equation it is possible to calculate the rate constant for cyclization of α,γ-hydroperoxyalkyl radicals for our temperature range as equal to $1.5\text{–}5.5 \times 10^3\ s^{-1}$. Comparing these estimated values to the rates of competing reactions 2′ and −4 predicts that concentrations of disubstituted oxetanes produced by reaction 10-α,γ would be less than 10^{-5} M under our conditions. These values are below the detection limits of our analytical procedures. Mill[20] reported Arrhenius parameters for α,γ cyclization of a tertiary radical from oxidation of 2,4-dimethylpentane in the liquid phase at 100 °C. The activation energy in that case was 3.5 kcal/mol less than that estimated from the gas-phase data for secondary radicals.

(18) Bastow, A. W.; Cullis, C. F. *Proc. R. Soc. London, A* **1974**, *341*, 195.
(19) Knox, J. H.; Kinnear, C. G. In *13th Int. Combustion Symposium*; The Combustion Institute: Pittsburgh, PA, 1977; p 217.
(20) Mill, T. In *13th Int. Combustion Symposium*; The Combustion Institute: Pittsburgh, PA, 1971; p 237.

Solvophobic and Entropic Driving Forces for Forming Velcraplexes, Which Are Four-Fold, Lock-Key Dimers in Organic Media[1,2]

Donald J. Cram,* Heung-Jin Choi, Judi A. Bryant, and Carolyn B. Knobler

Contribution from the Department of Chemistry and Biochemistry, University of California, Los Angeles, Los Angeles, California 90024. *Received March 2, 1992*

Abstract: Systems have been prepared composed of aromatic groups rigidly arranged to form ~15 by ~20 Å rectangular surfaces containing two regularly spaced protruding methyls at 3 and 9 o'clock and two methyl-sized holes at 12 and 6 o'clock (e.g., **1**). These molecules form dimers with large common surfaces in which the four methyl groups insert into the four holes. The resulting complexes have 82 to 132 intermolecular atom-to-atom contacts at van der Waals distances +0.2 Å (five crystal structures). Substitution of ethyls or hydrogens for the central aryl methyls eliminates complexation. Eight substituents attached at the periphery of the monomers extend the surfaces and profoundly affect the binding free energies ($-\Delta G°$ values) of the complexes, which range from <1 to >9 kcal mol^{-1} in $CDCl_3$ at temperatures −30 to 25 °C. Peripheral substituents with rotational degrees of freedom inhibit homodimerization. Activation free energies ($\Delta G^{\ddagger}$) for five dimerizations ranged from 8 to 10 kcal mol^{-1} and for five dissociations from 10 to 15 kcal mol^{-1} (in $CDCl_3$), suggesting their transition states to be very poorly solvated. The $-\Delta G°$ values for dimerization with notable exceptions increased dramatically with solvent polarity and polarizability. Enthalpies (ΔH values) ranged from +6 to −8 kcal mol^{-1} and entropies (ΔS values) from −6 to +40 cal mol^{-1} K^{-1}. Some dimerizations were entropy driven and enthalpy opposed, pointing to large solvophobic effects in organic media.

This paper reports the results of a study of complexation between two molecules, each of which possesses both host and guest character.[3] The complexing partners are highly preorganized[4] for complexation in such a way that each possesses a large rectangular face approximately 15 by 20 Å containing two protruding "up" methyls at 3 and 9 o'clock and two methyl-sized cavities at 12 and 6 o'clock lined by a sloping aryl face, an "out" methyl, and two oxygens. Prototypical structure **1a**, when rotated 90° about an axis normal to the page, gives view **1b**, which when turned over and placed on top of **1a**, beautifully forms a complex containing a large surface common to each partner, locked together by four methyl groups fitting into four cavities. In CPK models of the complex **1·1**, the monomers can neither slip nor rotate with respect to one another because of the four methyl locks. The dimerization is illustrated by A + B → C in the simplified drawings. In models of **1·1**, four sets of the quinoxaline "wings" contact one another, with their inner six-membered rings lying face-to-face.

All of the systems of this paper contain four conformationally mobile pentyl groups located on the side of each monomer opposite the complexing face. These "feet" provide monomer and dimer with the solubility in organic solvents required for this study. Models of **1·1** suggest to the viewer a globular jelly fish containing eight tentacles. Complexing systems **1** and **4–18** are further characterized by the absence in their structures of hydrogen bonds, ion pairs, or metal ligation sites common to many stable complexes. This leaves dipole–dipole, van der Waals, and solvophobic attractions as driving forces for complexation.

An earlier paper reported the synthesis of quinoxaline dimer **1·1** and quinoxaline monomers **2** and **3** as well as pyrazine dimer **4**.[5] Noncomplexing compound **3** is conformationally mobile, existing in a vase (C_{4v}) conformation (**3a**) at 25° and above, and in a kite (C_{2v}) conformation (**3b**) similar to that of **1a** at temperatures below −50 °C. The arylmethyls of **1** and arylethyls of **2** sterically inhibit formation of the vase conformations but undergo

(1) Host–Guest Complexation. 62.
(2) We warmly thank the U.S. Public Health Service for supporting Grant GE-12640.
(3) Two communications have appeared which collectively describe a small fraction of the work reported here: (a) Bryant, J. A.; Knobler, C. B.; Cram, D. J. *J. Am. Chem. Soc.* **1990**, *112*, 1254. (b) Bryant, J. A.; Ericson, J. L.; Cram, D. J. *J. Am. Chem. Soc.* **1990**, *112*, 1255.
(4) Cram, D. J. *Angew. Chem. Int. Engl. Ed.* **1986**, *25*, 1039–1057.
(5) Moran, J. R.; Ericson, J. L.; Dalcanale, E.; Bryant, J. A.; Knobler, C. B.; Cram, D. J. *J. Am. Chem. Soc.* **1991**, *113*, 5707–5714.

0002-7863/92/1514-7748$03.00/0

Scheme I

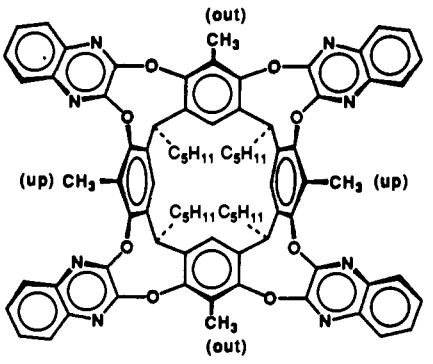

1a (C_{2v}), or HQx

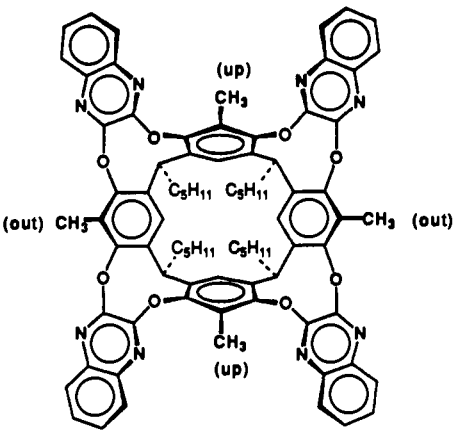

1b ($C_{2v'}$)

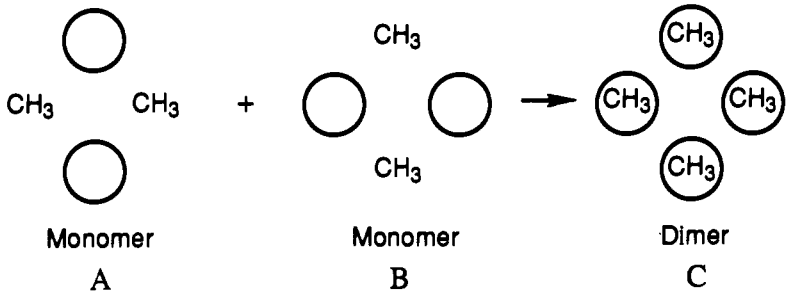

degenerate equilibrations between two identical kite structures such as **2a** and **2b** ($C_{2v} \rightleftarrows C_{2v'}$). The activation free energies ($\Delta G^{\ddagger}$, kcal mol^{-1}) for this equilibration of **2** were ~17.8 (T_c, 100 °C) in $CDCl_2CDCl_2$ and ~15.3 (T_c, 42 °C) in $C_6D_5CD_3$; those for the methyl-footed homologue of **1** were ~17–18 (T_c, 100 °C) in $CDCl_3$ and ~18–19 kcal mol^{-1} (T_c, 130 °C) in $(CD_3)_2SO$. The T_C value for chloropyrazine **4** in $C_6D_5CD_3$ was 70 °C. These T_c temperatures are well above those employed in the current paper, which focuses on the homodimerizations and heterodimerizations of **1** and **4–20**. At the temperatures employed in the present study, the conformational mobility of the monomers can be disregarded. We propose the terms velcrands and velcraplexes for these compounds whose molecules stick to one another.

Results

Syntheses. All of the velcrand syntheses reported here involve as their key step the condensation of haloaromatic compounds **21–32** with octol **33**.[6] An improved synthesis of octol **33** from 2-methylresorcinol and hexanal provided an 81% yield of this important starting material. Halides **21–32** have in common two vicinal halogens substituted in aromatic rings which readily undergo nucleophilic aromatic substitution reactions. As applied to the 12 reactions between **33** and **21–32**, each involves the making and breaking of eight bonds between oxygen and aryl carbons to produce four new nine-membered rings. Remarkably high yields were obtained which usually ranged between 50 and 86% for these reactions, whose products were easily isolated. Lower yields for preparing **8** (36%) and **15** (31%) were exceptions.

When 6 mmol of **21** was condensed with 2 mmol of **33**, a mixture of products was obtained which was easily separated chromatographically to give **1** (41%), **20** (30%), and two tetrols, syn (6%) and anti (4%), the latter two compounds being characterized only by ^{1}H NMR and FAB MS (see Experimental Section).

Compounds **21** and **23** are commercially available, and **22**,[7] **24**,[13] **25**,[8] **26**,[9] **28**,[11,12] **29**,[11] **31**,[10] and **32**[11] were prepared as previously reported, whereas **27** and **30** are new compounds. Diethylpyrazine (**27**) was prepared by a sequence that was analogous to the preparation of dimethylpyrazine **26** (see Experimental Section). In the synthesis of **30**, 2,3-dichloroquinoxaline (**21**) was oxidized ($KMnO_4$)[14] to give 2,3-dichloropyrazine-5,6-dicarboxylic acid. This diacid when mixed with $SOCl_2$ gave the corresponding anhydride, which when heated with CH_3NH_2–HCl in Ac_2O gave imide **30**.

Most of the remaining new velcrands were prepared from those already synthesized. The eight fluorine atoms in **8** were readily substitutable by strong nucleophiles. Treatment of **8** with $NaOCH_3$–$(CH_3)_2NCHO$ gave **9** (83%), with $NaSCH_3$–$(CH_3)_2NCHO$ gave **10** (67%), with $(CH_3)_2NH$-K_2CO_3–$[(CH_3)_2N]_3PO$ gave **11** (55%), and with CH_3NH_2–$(CH_3)_2NCHO$ gave **19** (47%). The number of fluorine atoms substituted in **19** was determined by elemental analysis, and the substitution pattern by ^{1}H, ^{13}C, and ^{19}F NMR spectra and by crystal structure determination. The lack of reactivity of the four last fluorine atoms toward nucleophilic

(6) Tunstad, L. M.; Tucker, J. A.; Dalcanale, E.; Weiser, J.; Bryant, J. A.; Sherman, J. C.; Helgeson, R. C.; Knobler, C. B.; Cram, D. J. *J. Org. Chem.* **1989**, *54*, 1305–1312.

(7) (a) Woolley, D. W.; Stewart, J. M. *J. Med. Chem.* **1963**, *6*, 599–601. (b) Stevens, J. R.; Pfister III, K.; Wolf, F. J. *J. Am. Chem. Soc.* **1946**, *68*, 1035–1039.

(8) (a) Erickson, A. E.; Spoerri, P. E. *J. Am. Chem. Soc.* **1946**, *68*, 400–402. (b) Adachi, J.; Sato, N. *J. Org. Chem.* **1972**, *37*, 221–225.

(9) (a) Karmas, G.; Spoerri, P. E. *J. Am. Chem. Soc.* **1952**, *74*, 1580–1584. (b) Karmas, G.; Spoerri, P. E. **1956**, *78*, 4071–4077.

(10) (a) Allison, C. G.; Chambers, R. D.; MacBride, J. A. H.; Musgrave, W. K. R. *J. Chem. Soc. (C)* **1970**, 1023–1029. (b) Jones, R. G.; McLaughlin, K. C. *Org. Synth.* **1963**, *4*, 824–827.

(11) (a) Donald, D. S. (duPont de Nemours, E. I., and Co.) U.S. 3,879,394, 1975. (b) Bredereck, H.; Schmötzer, G. *Justus Liebigs Ann. Chem.* **1956**, *600*, 95–108.

(12) Kazimierczuk, Z.; Dudycz, L.; Stolarski, R.; Shugar, D. *J. Carbohydr. Nucleosides, Nucleotides* **1981**, *8*, 101–117.

(13) Cheezeman, G. W. H. *J. Chem. Soc.* **1962**, 1170–1176.

(14) See (a) Elina, A. S.; Mustatova, I. S. *Chem. Heterocyclic Comp.* **1973**, *9*, 1403–1406. (b) Mager, H. I. X.; Berends, W. *Recl. Trav. Chim.* **1958**, *77*, 842–849.

Scheme II

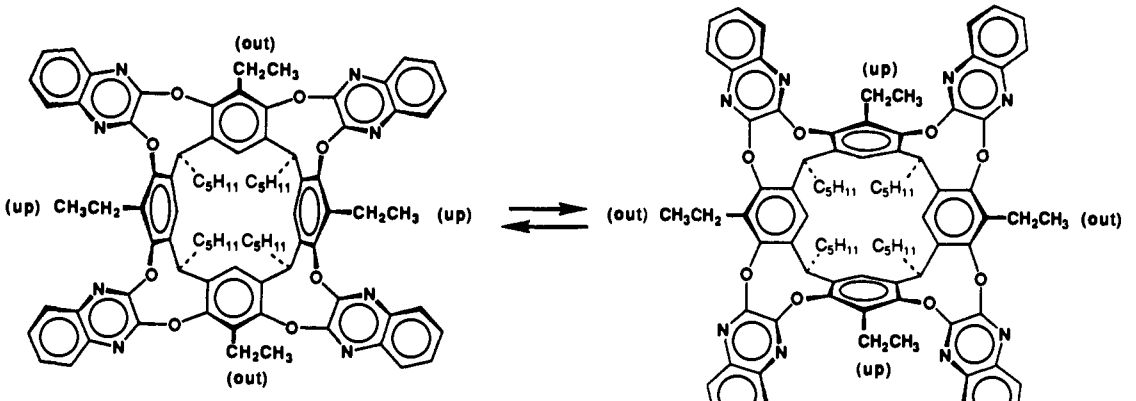

2a (C_{2v}) **2b** ($C_{2v'}$)

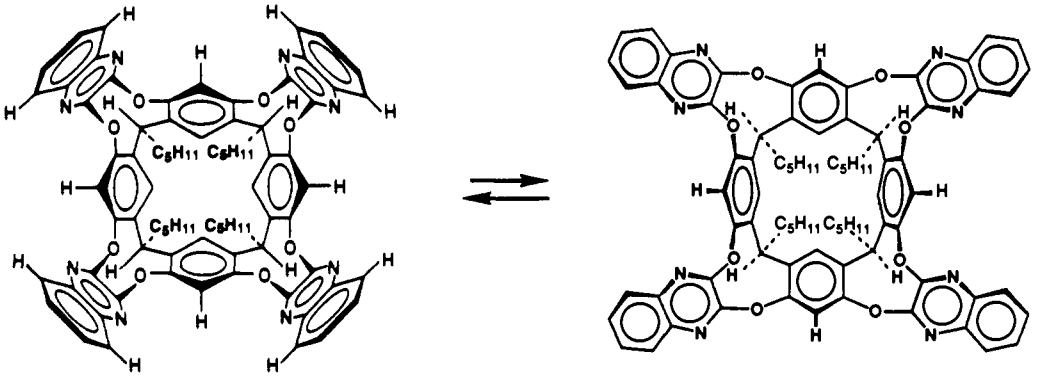

3a, vase (C_{4v}) **3b**, kite (C_{2v})

attack is explained by the existence of the molecule in the tautomeric form indicated by E or to the existence of **19** as a tetraanion suggested by F, whose charge is highly delocalized. The construction of CPK models of regioisomers of **19** indicate them to be much more sterically hindered due to encroachment of proximate $NHCH_3$ groups on one another's space.

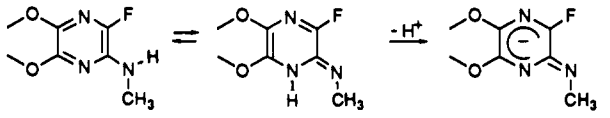

D E F

Velcrand **18**, containing four cyclic urea units, was synthesized from **17** by a five-step process (11% overall yield), the intermediates of which were characterized only by their NMR spectra. Reduction of the eight NO_2 groups of **17** with $SnCl_2$–HCl–EtOH gave the corresponding octaamine, which was tosylated in pyridine with p-$CH_3C_6H_4SO_2Cl$. The resulting octatosylamide was alkylated with CH_3I–K_2CO_3–$(CH_3)_2NCHO$ to provide the octa-*N*-methyl tosylamide, whose tosyl groups were removed by reduction with sodium anthracenide in $(CH_2)_4O$ to give the octa-*N*-methylamine. This material was converted to tetraurea **18** by treatment with triphosgene–Et_3N–$(CH_2)_4O$.

We refer to the pyrazine velcrands by the Pz abbreviation, to the quinoxaline by the Qx abbreviation, and to the benzene by the Bz abbreviation, with their substituent types as prefixes. These short names are placed beside the compound numbers below the formulas.

Crystal Structures. We report here the crystal structures of dimers **1·1**, **4·4**, **5·5**, **6·6**, **19·19**, and monomer **2**. Crystallization of **1·1** from acetone gave **1·1**·6(CH_3COCH_3), whose acetone was disordered, R = 0.166. Crystallization of **2** from EtOAc–$C_6H_5NO_2$–CH_2Cl_2–$CHCl_3$ gave **2**·EtOAc, whose EtOAc was disordered, R = 0.12. Crystallization of **4·4** from $C_6H_5NO_2$ gave **4·4**·8$C_6H_5NO_2$, some of whose $C_6H_5NO_2$ molecules were disordered, R = 0.12. Crystallization of **5·5** from $CH_3C_6H_5$ gave **5·5**·$n$$C_6H_5CH_3$ in which $n \approx 9$, none of whose solvate molecules were characterizable due to their disorder, R = 0.22. Crystallization of **6·6** from $C_6H_5NO_2$ gave **6·6**·$n$$C_6H_5NO_2$ in which $n >$ 7, since more uncharacterizable molecules are present in the crystal, which is ~1/3 solvent, R = 0.25. Compound **19·19** was crystallized from CH_2Cl_2–CH_3NO_2 to give **19·19**·2 (solvent, un-

Table I. Short Intermonomer Atomic Distances in Crystalline Dimers

kinds of atoms	distance less than (Å)	no. of short distances in dimers				
		1·1	**4·4**	**5·5**	**6·6**	**19·19**
H···H	2.7	32	7	8	18	8
N···H	3.0	0	0	9	7	4
C···H	3.2	58	17	27	46	16
O···H	3.0	10	11	15	9	8
C···N	3.5	6	8	10	6	14
C···O	3.5	8	8	8	8	8
N···O	3.3	0	0	0	0	0
C···C	3.7	18	24	7	13	22
O···O	3.3	0	0	0	0	0
Cl···N	3.6	0	4	0	0	0
Cl···H	3.3	0	3	0	0	0
Cl···C	3.7	0	3	0	0	0
Cl···O	3.6	0	1	0	0	0
F···N	3.4	0	0	0	0	2
C···F	3.5	0	0	0	0	0
F···H	3.0	0	0	0	0	0
total close distances		132	86	84	107	82

Chart I

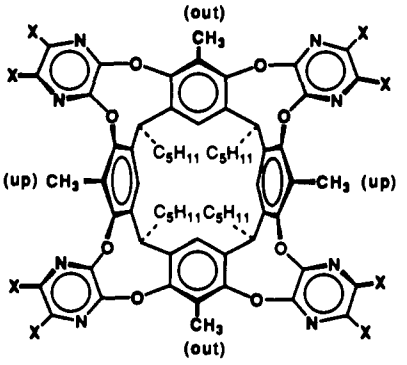

4, X = Cl,or ClPz
5, X = H, or HPz
6, X = CH_3, or MePz
7, X = CH_3CH_2, or EtPz
8, X = F, or FPz
9, X = OCH_3, or MeOPz
10, X = SCH_3, or MeSPz
11, X = $N(CH_3)_2$, or Me_2NPz
12, X = CN, or CNBPz

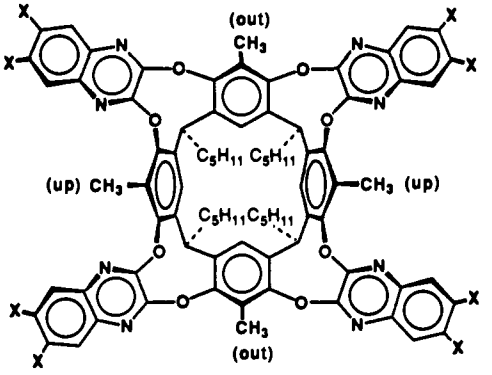

13, X = CH_3, or MeQx
14, X = Cl, or ClQx
15, X = Br, or BrQx

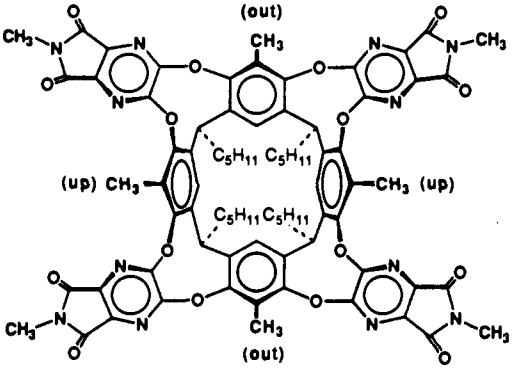

16, or ImidePz

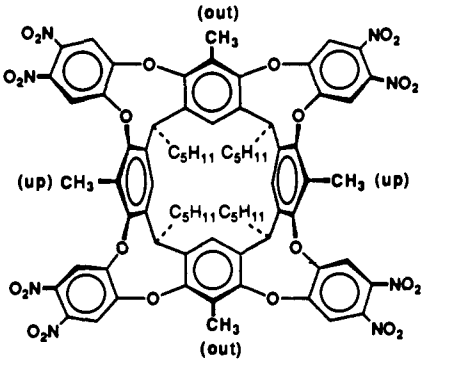

17, or NO_2Bz

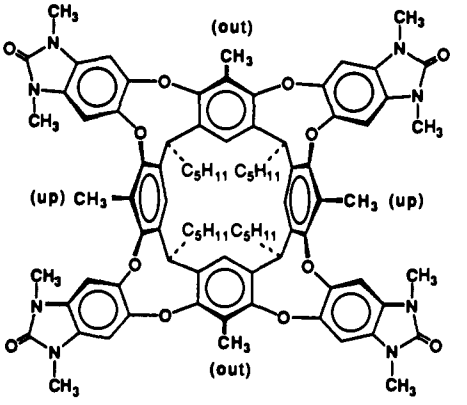

18, or UreaBz

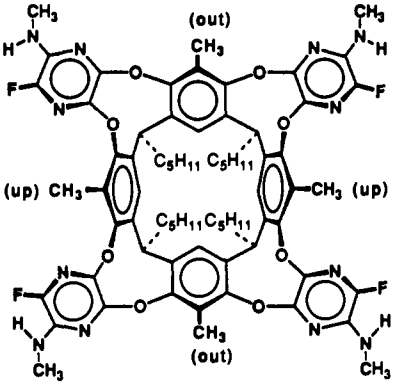

19, or FMeNPz

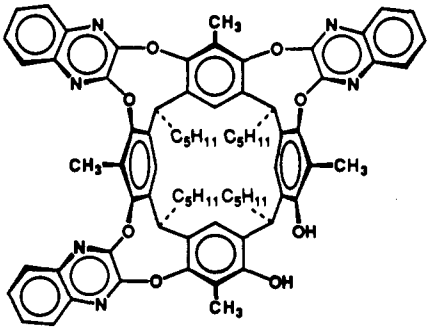

20, or $(HO)_2Qx$

Chart II

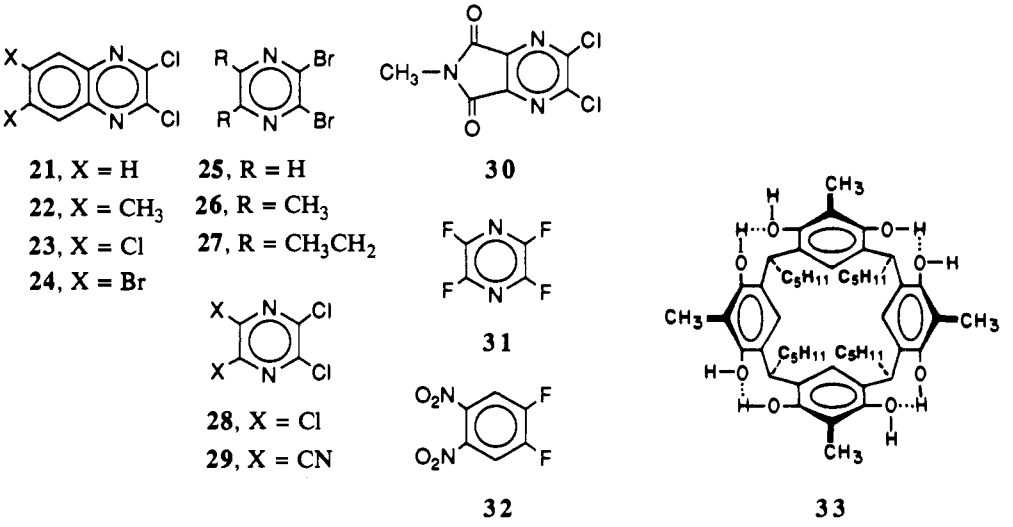

identified), $R = 0.23$. Although the degree of refinement of these structures is lower than desirable, the sizes of the unit cell are large, and the numbers of disordered solvent molecules inhibit refinement. In the crystal structure of **5·5**, the atoms of the pentyl groups most distant from the central globe were disordered and not located. Repeated attempts to obtain better crystals failed. However, the purpose of this paper is served by the data obtained. Chart III records face and side stereoviews of the six crystal structures, coupled with the kitelike structural formulas of the monomer units involved.

A main reason for determining these crystal structures was to obtain the numbers of short interatomic, nonbonded distances across the surfaces common to each monomer unit in the dimers. Table I identifies the kinds of close atoms, sets limiting distances for their being counted, the numbers of short distances for each kind of contact, and the sums of these short contacts for each dimer.

Molecular Weight of Equilibrating Kinds of 1 and 4 in Solution. Vapor pressure osmometric molecular weight determinations of **1** (HQx) (10.9–40 mM concentrations) at 27 °C gave values of 2783 ± 280, close to that of dimer (**1·1**, 2658). A similar determination for **4** (ClPz) (7.8–31 mM concentrations) gave molecular weights of 2665 ± (270), much closer to that of dimer (**4·4**, 2808) than that of monomer (**4**, 1404). The best criterion of molecular weight in solution came from ^{1}H NMR spectral determinations (see future sections).

Spectral Evidence for Dimerization. In $CDCl_3$ at −18 °C, the 360-MHz ^{1}H NMR spectrum of monomer **4** (ClPz) gave δ 2.19 for the two up methyls and δ 2.43 for the two out methyls, whereas these respective signals move to δ 1.69 and 2.63 in the dimer. Irradiation of the δ 2.63 peak (500 MHz at −18 °C) produced −3% enhancements of the δ 1.69 peak. Irradiation of the δ 1.69 peak was unfruitful because it was partially obscured by adventitious water signals.[15] Control irradiations of aryl protons gave −3 to −10% enhancements. Negative enhancements are frequently encountered in large molecules.[16]

The equilibrium between monomer and dimer is highly dependent on concentration and temperature, so the ratios of dimer to monomer were changed by varying these conditions. In some systems, homodimerization was so weak (EtPz, MeOPz, CNPz, MeSPz, Me_2NPz, NO_2Bz), dimer could not be detected, whereas with UreaBz, only dimer could be detected. Table II lists the chemical shifts for monomers and dimers in representative systems HPz, MePz, HQx, and MeQx. Note that the signals for (up) $CH_3{}^b$ protons in the dimers are all *upfield* of those of the monomer by $\Delta\delta = 0.45$ ppm for HPz and MePz, by $\Delta\delta = 0.29$ ppm for HQx, and 0.35 ppm for MeQx. The crystal structures of all of the dimers show these up methyl groups to be located in the shielding region of the tilted benzene rings which line the four cavities of the complexing partners. The $\Delta\delta$ values for (out) $CH_3{}^a$ protons in these dimers are all *downfield* of those for monomers by amounts that range from 0.03 ppm for HPz to 0.46 ppm for MeQx. These (out) methyls generally lie in the deshielding region of the complexing partners in CPK molecular models. The H^c protons are distant from the complexing faces and provide $\Delta\delta$ values that vary only from 0.01 to 0.08 ppm for the four systems. The aryls' H^c protons are all tilted inward toward one another and are moved *upfield* by 0.70 to 0.92 ppm by the shielding cone of their two adjacent benzene rings, as compared to the aryls' H^d protons, which are wedged between the methylenes of the pentyl appendages. For reasons not understood, the signals of these H^d protons in the dimer are *upfield* of those for the H^d protons of the monomer by 0.16 to 0.23 ppm. Likewise, the methines' H^e proton signals in the dimer are *upfield* of those in the monomer by 0.16 to 0.25 ppm. The H^h protons of HPz dimer lie slightly over their complexing partner's aryls and are more *upfield* by 0.62 ppm compared to the H^h protons of the monomer. The H^i protons of the monomer and dimer possess the same chemical shift in HPz. The $CH_3{}^j$ and $CH_3{}^k$ signals of MeQx dimer and monomer hardly differ from one another. The H^c protons of HQx dimer are *upfield* of those of the monomer by $\Delta\delta = 0.22$, again being affected by the shielding cones of the complexing partner's aryl groups. The H^l, H^m, H^n, and H^o signals of HQx monomer were too complex to be useful.

The UV spectra of several systems were determined as a function of concentration in the hope of detecting analytically useful charge-transfer bands present in the dimer but absent in the monomer. None were detected. In CH_2Cl_2, UreaBz (**18**) gave $\lambda_{max} = 229$ nm (log $\epsilon = 5.04$) and $\lambda_{max} = 311$ nm (log $\epsilon = 4.65$), invariant from 2.74×10^{-6} to 4.39×10^{-7} M concentration. In CH_2Cl_2, ImidePz (**16**) gave $\lambda_{max} = 229$ nm (log $\epsilon = 4.79$) and $\lambda_{max} = 316$ nm (log $\epsilon = 4.65$), invariant from 1.37×10^{-4} to 1.37×10^{-6} M. In CH_3CN, HQx (**1**) gave $\lambda_{max} = 203$ nm (log $\epsilon = 5.50$), 246 nm (log $\epsilon = 5.18$), 328 nm (log $\epsilon = 4.68$), and 340 nm (log $\epsilon = 4.68$), invariant from 1.37×10^{-4} to 1.37×10^{-6} M.

Equations Used in Determinations of Association Constants for Homo- and Heterodimerizations. The association–dissociation rates for the respective monomers (M) and dimers (D) at temperatures between +30 °C to −50 °C were usually slow on the ^{1}H NMR time scale[17] (see future section). Thus the populations of M and D were determined directly by integration of their respective peaks, which provided a convenient means of determining the association constants (K_a, M^{-1}). In equation 1, for

(15) We thank Michael Geckle for help with the NOE experiments.
(16) Derome, A. E. *Modern NMR Techniques for Chemical Research*; Pergamon Press; Oxford, 1987.
(17) Johnson, C. S., Jr. *Advances in Magnetic Resonance*; Waugh, J. S., Ed.; Academic Press: London, 1965; Vol. 1, pp 33–102.

Table II. Chemical Shift (δ) Comparisons of Selected Signals in the ^{1}H NMR Spectra of Four Velcrands and Their Corresponding Velcraplexes

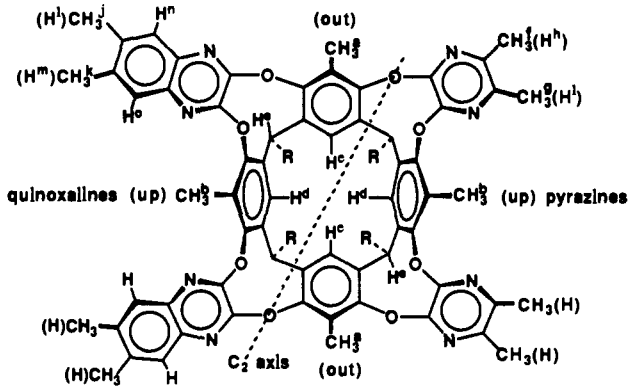

5, **6**, **1**, and **13**

δ of protons	**5**[a] (HPz)		**6**[b] (MePz)		**1**[c] (HQx)		**13**[d] (MeQx)	
	dimer	monomer	dimer	monomer	dimer	monomer	dimer	monomer
$CH_3{}^a$	2.47	2.44	2.68	2.48	3.16	2.66	3.11	2.65
$CH_3{}^b$	1.62	2.07	1.84	2.29	2.23	2.52	2.13	2.48
H^c	5.95	6.03	6.03	6.04	6.17		6.10	6.15
H^d	6.73	6.95	6.82	6.98	6.87		6.82	7.05
H^e	3.38	3.57	3.61	3.77	3.52	3.76	3.50	3.75
$CH_3{}^f$			2.21	2.34				
$CH_3{}^g$			2.39	2.48				
H^h	7.50	8.12						
H^i	7.89	7.89						
$CH_3{}^j$							2.43	2.47
$CH_3{}^k$							2.61	2.61
H^l					7.46			
H^m					7.67			
H^n					7.16		6.84	?
H^o					7.80		7.51	7.73

[a] 20 mM in CD_2Cl_2 at −80 °C. [b] 1 mM in $CDCl_3$ at 0 °C. [c] 0.05 M in $CDCl_3$ at −10 °C. [d] 0.50 mM in $CDCl_3$ at −20 °C.

homodimerization, R = 0.5 (integral value of dimer)/(integral value of monomer), and $[M]_i$ is the initial concentration of monomer.

$$M + M \rightleftarrows D \qquad K_a = R(2R + 1)/[M]_i \tag{1}$$

Heterodimerization experiments between monomer A (M_A) and B (M_B) leading to dimer AB (D_{AB}) were conducted by mixing equal molar amounts of A and B. The new ^{1}H NMR signals not present in the spectra of the two separated monomers or their dimers (D_A and D_B) were assigned to the heterodimers, D_{AB}. The most useful signals were those due to the Ar-H, methine, or Ar-CH_3 protons. Equations 2–4 were derived from the mass balance of each species in the system. Generally, it was convenient

$$M_A + M_B \rightleftarrows D_A + D_B + D_{AB} \tag{2}$$

$$K_{DA} = [D_A]/[M_A]^2, \qquad K_{DB} = [D_B]/[M_B]^2, \qquad K_{DAB} = [D_{AB}]/([M_A][M_B]) \tag{3}$$

$$[D_{AB}] = [M_A]_i - 2[D_A] - [M_A] = [M_B]_i - 2[D_B] - [M_B] \tag{4}$$

to define R_{AB} as the ratios of integral values of D_{AB} over the sum of the integrals of the related components, as shown in eq 5.

$$R_{AB} = [D_{AB}]/\{2[D_A] + [D_{AB}] + [M_A]\} = [D_{AB}]/\{2[D_B] + [D_{AB}] + [M_B]\} \tag{5}$$

In the case of strong dimerization of monomer A, $[M_A] \approx 0$, and eqs 6 and 7 apply.

$$R_{AB} = [D_{AB}]/(2[D_A] + [D_{AB}]) = \text{integral of } D_{AB}/\{\text{integral of } D_A + \text{integral of } D_{AB}\} \tag{6}$$

$$[D_{AB}] = R_{AB}[M_A]_i \tag{7}$$

Usually the M_A and M_B signals were too small to integrate, but were calculated from $[M_A]_i$, $[M_B]_i$, the temperature, and K_{DA} and K_{DB} obtained from homodimerization experiments, where $R_A = [D_A]/[M_A]$ and $R_B = [D_B]/[M_B]$. Use was made of eqs 8, 9, and 10. To calculate C, $[M_A]_i$ was used as the initial concentration of monomer A, although it should be less than

$$K_{DA} = \{R_A(2R_A + 1)\}/[M_A]_i = e^{-(\Delta G/RT)} \tag{8}$$

$$2R_A{}^2 + R_A - K_{DA}[M_A]_i = 0 \tag{9}$$

$$R_A = (-1 + \sqrt{1 + 8C})/4 \text{ where } C = K_{DA}[M_A]_i \tag{10}$$

the initial concentration of A due to heterodimerization. However, the final K_{DAB} value is not sensitive to the initial concentration of A.

In the cases in which $[M_A]$ and $[M_B]$ could not be measured directly from the ^{1}H NMR spectra, they were calculated using eqs 11.

$$[M_A] = \{[M_A]_i - [D_{AB}]\}/(1 + 2R_A) \qquad [M_B] = \{[M_B]_i - [D_{AB}]\}/(1 + 2R_B) \tag{11}$$

For strong heterodimerization in which only D_{AB} is observable, we assumed D_A and D_B as $[D_A] \approx [D_B] < (0.1[M]_i)$, and M_A and M_B as $[M_A] \approx [M_B] = 0$. The calculated $[M_A]$ and $[M_B]$ values were then used to set lower limits for K_{DAB} and $\Delta G°$.

When neither monomers A nor B homodimerize but heterodimerize, the new signals due to heterodimer D_{AB} and those due to M_A and M_B were directly integrated. The treatment shown in eq 12 resembles that for homodimerization.

$$K_{DAB} = \{R_{AB}(R_{AB} + 1)\}/[M_A]_i = \{R_{AB}(R_{AB} + 1)\}/[M_B]_i, \text{ where } R_{AB} = [D_{AB}]/[M_A] = [D_{AB}]/[M_B] \tag{12}$$

Thermodynamic Parameters. To obtain $\Delta G°$, ΔH, and ΔS values for the dimerizations, a series of association constants (K_a) were determined over a range of temperatures between +20 °C

Chart III. Line Structures of Monomers and Crystal Structures of Monomers and Dimers

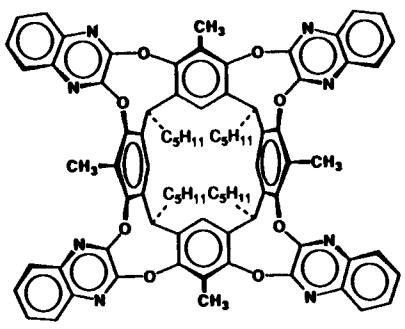

1

top view

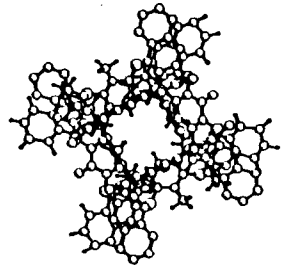

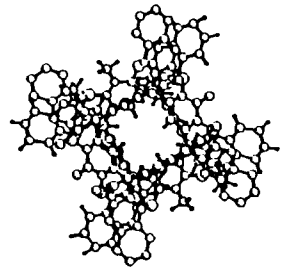

side view

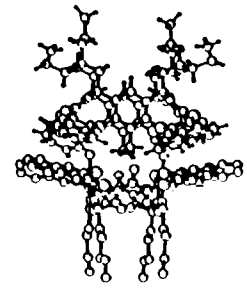

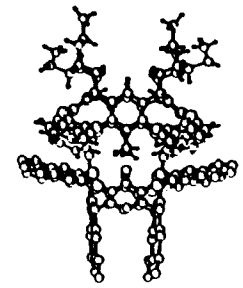

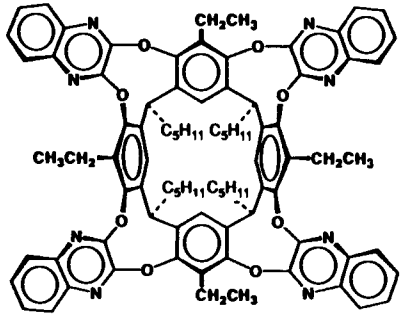

2

bottom view

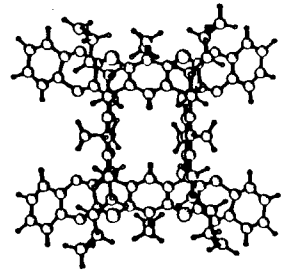

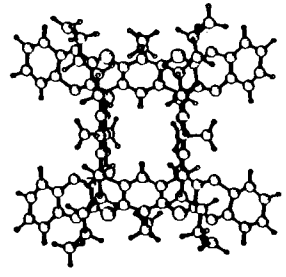

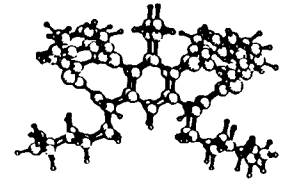

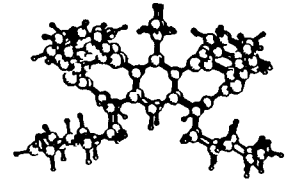

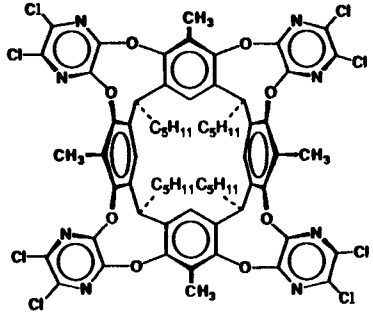

4

top view

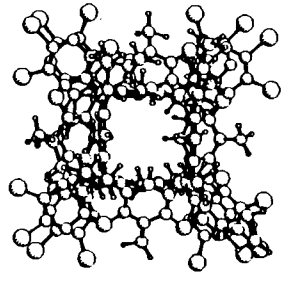

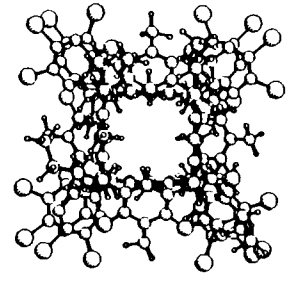

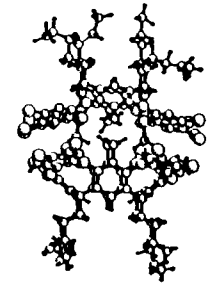

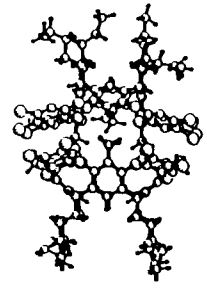

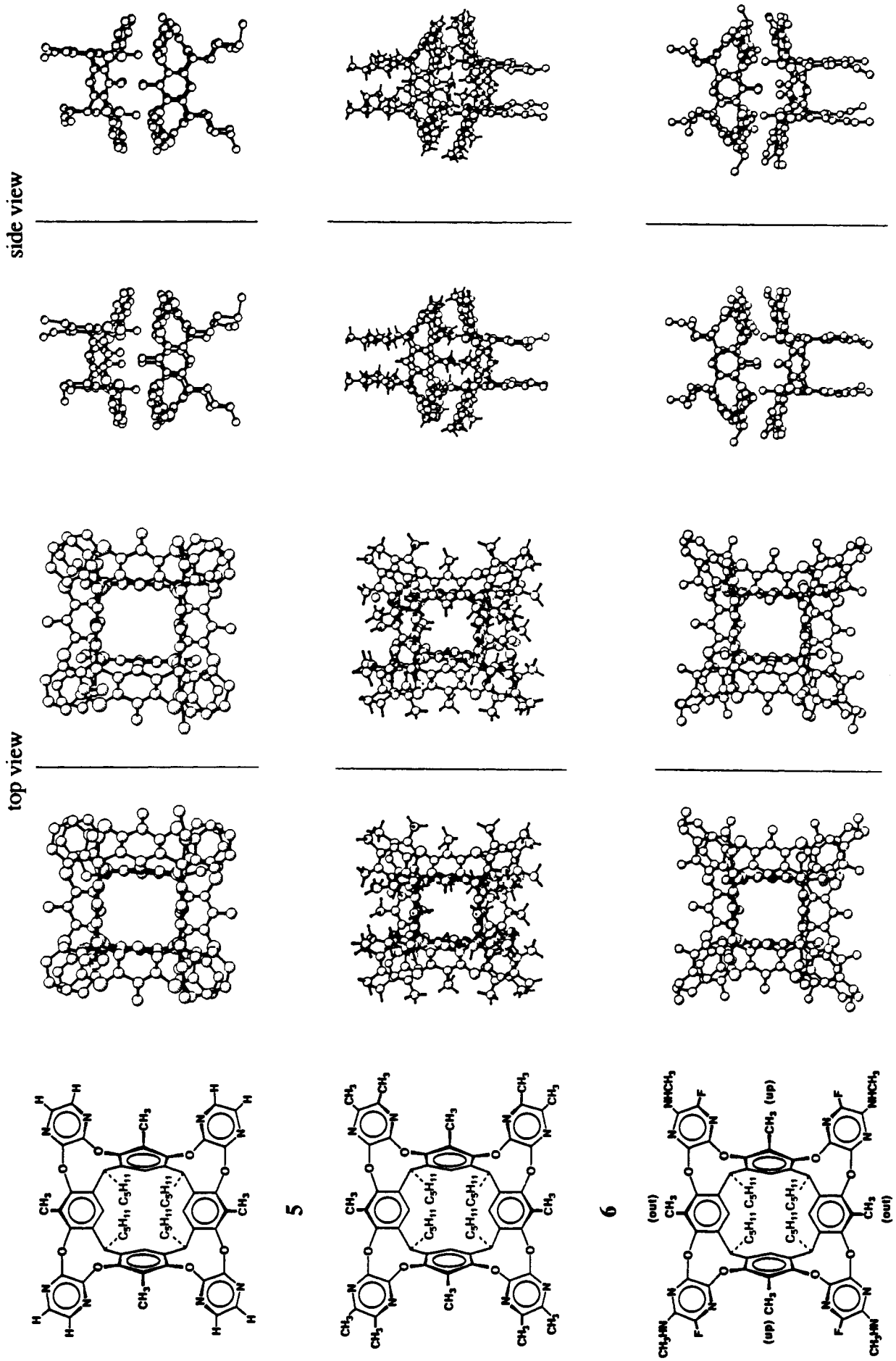
side view
top view
5
6
19

and −50 °C. Values of $-\Delta G°$ were calculated using eq 13, ΔH values were obtained from van't Hoff plots, and ΔS from eq 14.

$$-\Delta G° = RT \ln K_a \quad (13)$$

$$\Delta S = (\Delta H - \Delta G°)/T \quad (14)$$

Homodimerization. Table I in the supplementary material records the temperatures, concentrations, and association constants (K_a) for homodimerizations in $CDCl_3$ as measured on a 500-MHz ^1H NMR machine. Values are reported for ClPz at 1.0 mM initial concentration for six temperatures (263–227 K); for HPz at 20 mM for six temperatures (203–178 K); for CH_3Pz at 1.0 mM for six temperatures (283–233 K); for ImidePz at 0.1 mM for six temperatures (263–223 K), and at 1.0 mM for five temperatures (263–223 K); for HQx at 0.1 mM for eight temperatures (303–233 K); for MeQx at 0.05 mM at five temperatures (293–253 K); for ClQx at 0.1 mM at eight temperatures (303–233 K); for BrQx at 0.5 mM at five temperatures (273–243 K).

Only dimer was observed for UreaBz (**18**) under the following conditions: 0.01 mM in $CDCl_3$ at +40 to −40 °C; 0.5 mM in $CDCl_3$ at +50 to −40 °C; 0.5 mM in $(CD_3)_2CO$ at +50 to −50 °C; 0.5 mM in CD_2Cl_2-$CDCl_3$ (2:1, v) or CD_2Cl_2-$CDCl_3$ (9:1, v) at −115 °C. Only dimer was observed for $(HO)_2Qx$ (**20**) at 0.05 mM in $CDCl_3$ at +40 to −50 °C. If [D]/[M] > 9, then $K_a > 3.4 \times 10^6$ M^{-1} and $-\Delta G° > 7.9$ kcal mol^{-1}.

No homodimer was observed for the following systems: EtPz (**7**), 10 mM in CD_2Cl_2 at −90 °C; FPz (**8**), 50 mM in CD_2Cl_2 at −90 °C; MeOPz (**9**), 20 mM in $CDCl_3$-$(CD_3)_2CO$ (1:1, v) at −70 °C; MeSPz (**10**), 10 mM in CD_2Cl_2 at −90 °C; Me_2NPz (**11**), 10 mM in CD_2Cl_2 at −90 °C; CNPz (**12**), 10 mM in $CDCl_3$ at −50 °C); FMeNPz (**19**), 20 mM in $CDCl_3$ at +20 to −40 °C; and NO_2Bz (**17**), 0.5 mM in $CDCl_3$ at +20 to −40 °C (limited solubility). We estimate that the $-\Delta G°$ values for homodimerization as small as 1 kcal mol^{-1} could have been measured.

Heterodimerization. Table II in the supplementary material reports the results for those pairs of different partners that bind one another. The footnotes identify the protons whose signals were used and the equations employed to calculate K_a. The dimers, their temperatures (K, number), and the initial concentrations (mM) of their monomers employed are (respectively) as follows: HPz·MePz, 273–233 (3), 1.0; HPz·ClPz, 253–273 (3), 1.0; HPz·HQx, 273–233 (3), 1.0; HPz·MeQx, 293, 1.0; HPz·ClQx, 293, 1.0; MePz·FPz, 273–233 (5), 1.0; MePz·ClPz, 293, 1.0; MePz·HQx, 293, 1.0; MePz·MeQx, 293–253 (3), 1.0; MePz·ClQx, 293–233 (4), 1.0; EtPz·FPz, 233–218 (4), 5.0; EtPz·ClPz, 263–233 (5), 1.0; EtPz·CNPz, 263–218 (8), 10.0; MeOPz·ClPz, 253–223 (4), 10.0; ClPz·HQx, 293–233 (4), 1.0; ClPz·MeQx, 293, 1.0; ClPz·ClQx, 293–233 (4), 1.0; HQx·MeQx, 293–233 (4), 1.0; HQx·ClQx, 293–233 (4), 1.0; MeQx·ClQx, 293, 1.0; NO_2Bz·MePz, 263–233 (4), 0.5; ImidePz·UreaPz, 263–223 (5), 0.5; ImidePz·HQx, 273, 1.0.

The UreaBz monomer was never detected in either homodimerization or heterodimer experiments, so there is no way to calculate its association constant. ImidePz dimer dissociates rapidly on the ^1H NMR time scale as shown by the fact that when mixed with HQx, it equilibrates with ImidePz·HQx. In further experiments with D_{UreaBz} and D_{HQx} in $CDCl_3$ with $[M]_i$ of each component at 1.0 mM concentration, a comparison was made between changes in the values of $[D_{UreaBz\cdot HQx}]/[D_{UreaBz}]$ and of $[D_{UreaBz\cdot HQx}]$ with 10 °C incremental changes in temperature. At 313–233 K $[D_{UreaBz\cdot HQx}]/[D_{UreaBz}]$ values decrease monotonically from 0.83 to 0.42, while $[D_{UreaBz\cdot HQx}]$ values decreased monotonically from 0.29 to 0.17. The homodimerization of HQx gave a ΔS value of −1.9 cal mol^{-1} K^{-1} and [D]/[M] ratios that changed from 1.34 at 303 K to 8.67 at 233 K. These results taken together indicate that the entropy for $D_{UreaBz\cdot HQx}$ formation has a substantially positive value and suggest further that D_{UreaBz} has an even larger positive entropy, possibly rivaling that of ImidePz at +40 cal mol^{-1} K^{-1}.

Attempts to form heterodimers in $CDCl_3$ at 223 K (10 mM concentrations of each component) from the following systems failed: MeOPz and FPz; MeOPz and MeSPz; MeOPz and Me_2NPz; FPz and ClPz; FPz and MeSPz; FPz and Me_2NPz; ClPz and MeSPz; ClPz and Me_2NPz; and MeSPz and Me_2NPz.

Table III. Association Constants, Free Energies, and Conditions for Dimerization of MePz in Various Solvents[a]

solvent	T (°C)	$[M]_i$ (mM)	K_a (× 10^3 M^{-1})	$-\Delta G°$ (kcal mol^{-1})	E_T (30)[b]
$(CD_2)_6$	25	1.0	>45.0	>6.34	30.9
CCl_4	0	1.0	2.5	4.25	32.4
$C_6D_5CD_3$	0	0.1	14.1	5.18	33.9
C_6D_6	10	1.0	5.7	4.82	34.3
C_6D_5Cl	0	1.0	7.3	4.82	36.8
$(CD_2)_4O$	0	0.1	14.2	5.19	37.4
$CDCl_3$	0	1.0	8.7	4.92	39.1
CD_2Cl_2	0	0.1	13.0	5.14	40.7
$(CD_3)_2CO$	0	0.01	>100	>6.3	42.2
$(CD_3)_2CO$	0–30	1.0	high	high	42.2
$(CD_3)_2NCDO$	0–25	1.0	high	high	43.8
CD_3CN	0	1.0	high	high	45.6
CD_3NO_2	0	1.0	high	high	46.3
CD_3CD_2OD	0	1.0	high	high	51.9
CD_3OD	0–30	1.0	high	high	55.4

[a] 500 MHz ^1H NMR spectrometer. [b] See ref 9. Values are for protonated solvents.

Table IV. Association Constants and Free Energies of Dimerization of ClPz in Various Solvents Compared to $CDCl_3$ as a Standard Solvent[a]

solvent[b]	T (°C)	$[M]_i$ (mM)	K_a[c] (×10^3 M^{-1})	$-\Delta G°$ (kcal mol^{-1})
$CDCl_3$[d]	25		1.0	4.1
$CDCl_3$	−18	1.0	3.1	4.1
$CDCl_3$	−46	1.1	7.1	4.0
CD_2Cl_2	−46	1.0	13	4.3
10% $C_6D_5CD_3$	−46	1.0	2.1	3.5
10% $C_6D_5CD_3$	−18	1.0	3.1	4.1
10% $(CD_3)_2CO$	−18	1.0	8.2	4.6
25% $(CD_3)_2CO$	−18	1.5	24	5.1
50% $(CD_3)_2CO$	−18	1.5	>110	>5.9
100% $(CD_3)_2CO$	−18	1.4	>120	>5.9
1% CD_3OD	−18	2.8	3.3	4.1
5% CD_3OD	−18	2.8	3.9	4.2
10% CD_3OD	−18	2.8	13	4.8
25% CD_3OD	−18	2.9	>59	>5.6
50% CD_3OD	−18	2.8	>61	>5.6
1% CD_3NO_2	−18	1.4	6.2	4.4
5% CD_3NO_2	−18	1.4	5.9	4.4
10% CD_3NO_2	−18	1.3	9.1	4.6
25% CD_3NO_2	−18	1.4	32	5.3
10% $(CD_2)_4O$	−18	1.0	5.2	4.3

[a] 360-MHz ^1H NMR spectrometer was used. [b] Mixed solvents were v/v% in $CDCl_3$. [c] Error ±20%. [d] Extrapolated from thermodynamic data.

Table V. Thermodynamic Parameters for Dimerization of ClPz in Three Media at 255 K[a]

solvent	ΔH (kcal mol^{-1})	ΔS (cal mol^{-1} K^{-1})	$-\Delta G°$ (kcal mol^{-1})
$CDCl_3$	−3.77	1.1	4.05
10% $(CD_3)_2CO$	−4.06	2.0	4.57
10% CD_3OD	−4.04	2.8	4.80

[a] 360-MHz ^1H NMR spectrophotometer, five point van't Hoff plots.

Solvent Effects on Dimerization. Because solvation of the large relatively flat surfaces of monomer competes directly with dimerization, we examined the effects of solvation on $-\Delta G°$ values for homodimerizations of MePz (enthalpy driven) and of ImidePz (entropy driven). Diederich and Smithrud[18] have shown that $-\Delta G°$ values in a wide range of solvents correlate linearly with E_T (30) values.[19] Fifteen solvents ranging from nonpolar cyclohexane (E_T (30) = 30.9) to polar methanol (E_T (30) = 55.4) were involved.[18] Table III records the K_a, $-\Delta G°$, and E_T (30) values, and the experimental conditions for dimerization of MePz in various solvents.

Table VI. Association Constants, Free Energies, Enthalpies, and Entropies for Homodimerization of ImidePz in Different Media at 1.0 mM Initial Concentration

temp (K)	K_a ($\times 10^3$ M^{-1})	$-\Delta G°$ (kcal mol^{-1})	ΔH (kcal mol^{-1})	ΔS (cal mol^{-1} K^{-1})	correl factor[a]
263[b]	1.39	3.78	5.07	33.7	−0.9975
253[b]	1.06	3.50			
243[b]	0.664	3.12			
233[b]	0.375	2.74			
223[b]	0.262	2.47			
213[b]	0.148	2.12			
293[c]	dimer	7.7[d]			
243[c]	186	5.86	3.34	37.8	−0.7325
233[c]	68.3	5.15			
223[c]	61.5	4.89			
213[c]	23.7	4.26			
203[c]	5.39	3.47			
193[e]	377	4.92			

[a] Correlation factors for points in the van't Hoff plot. [b] Solvent is CD_2Cl_2. [c] Solvent is CCl_4–CD_2Cl_2 (4/1, v/v). [d] Only dimer was detected; value is calculated from ΔH and ΔS. [e] From 30 °C to −50 °C; only dimer was detected; solvent is CD_2Cl_2–CD_3OD (1/1, v/v); initial concentration of ImidePz, 0.5 mM.

Table VII. Rate Constants and Activation Free Energies for Dimerization at Coalescence Temperatures in $CDCl_3$ with 500 MHz ^1H NMR Instrument

						at coalescence temperatures			
monomers	concn (mM)	signals coalesced	T_c (K)	$\Delta\nu$ (Hz)	K_a ($\times 10^3$ M^{-1})	k_d (s^{-1})	k_a ($\times 10^3$ M^{-1} s^{-1})	$\Delta G^{\ddagger}_d$ dissoc (kcal mol^{-1})	$\Delta G^{\ddagger}_a$ assoc (kcal mol^{-1})
HPz,HPz	20[a]	methine	213	93.72	0.106	208	22	10.05 ± 0.3	8.08 ± 0.3
ClPz,ClPz[b]	1.0	$ArCH_3$	285	47.9	1.3	106	140	14.0 ± 0.3	9.95 ± 0.3
FPz,EtPz[c]	5.0	methine	243	81	0.155	180	28	11.6 ± 0.3	9.17 ± 0.3
FPz,MePz	1.0	Ar-H	315	50[d]	6.91	111	767	15.5 ± 0.3	9.98 ± 0.3
ClPz,EtPz	1.0	Ar-H	273	53[d]	1.04	117	122	13.3 ± 0.3	9.57 ± 0.3

[a] CD_2Cl_2 was solvent. [b] 360-MHz ^1H NMR instrument was used. [c] Neither monomer dimerized, so process was treated like a homodimerization. [d] Half of the $\Delta\nu$ for the largest chemical shift difference was used since there were five Ar-H signals, two from monomers, two for heterodimer, and one for homodimer.

Table VIII. Velcraplex Existence in the FAB-MS (NOBA Matrix) Gas Phase

	molecular		obsd mass		% abundance		$\Delta G°(CDCl_3)$	temp
velcrand	formula	weight	monomr	dimer	monomr	dimer	(kcal mol^{-1})	(K)
FPz	$C_{68}H_{64}N_8O_8F_8$	1273 (1272)	1272		100	0	<1	
HPz	$C_{68}H_{72}N_8O_8$	1129 (1128)	1130		100	0	1.95	203
ClPz	$C_{68}H_{64}N_8O_8Cl_8$	1405 (1400)	1404	2807	100	0.6	4.05	263
MePz	$C_{76}H_{88}N_8O_8$	1242 (1240)	1242	2483	100	1.0	5.04	273
ImidePz	$C_{80}H_{76}N_{12}O_{16}$	1462 (1460)	1462	2923	100	3.0	5.29	263
UreaBz	$C_{88}H_{96}N_8O_{12}$	1458 (1456)	1458	2915	100	2.3	>8	273
HQx	$C_{84}H_{80}N_8O_8$	1330 (1328)	1330	2658	100	1.0	6.77	273
MeQx	$C_{92}H_{96}N_8O_8$	1442 (1440)	1442	2881	100	2.8	6.10	273
ClQx	$C_{84}H_{72}N_8O_8Cl_8$	1605 (1600)	1605	3210	100	2.0	6.22	273
BrQx	$C_{84}H_{72}N_8O_8Br_8$	1961 (1952)					5.62	273

In a second study involving ClPz, combinations of solvents were used to establish trends. The results are found in Table IV.

Table V records the thermodynamic parameters for ClPz in pure $CDCl_3$, and $CDCl_3$ mixed with $(CD_3)_2CO$ or CD_3OD. Both enthalpy and entropy favored dimerization as the medium became more polar.

Table VI gives the K_a, $-\Delta G°$, ΔH, and ΔS values for the ImidePz system in three media. In attempts to determine these same values in CCl_4–CD_2Cl_2 (9/1, v/v) from −40 to 70 °C and in CD_3OD–CD_2Cl_2 (1/1, v/v) from 30 to −50 °C, only dimer could be detected.

Kinetics of Dissociation of Dimer. The kinetic parameters for dissociation of dimer were measured by ^1H NMR temperature-coalescent methods.[20] Equations 15–17 apply to equally populated two-site exchange processes in which $\Delta G^{\ddagger}$ is the activation free energy for dissociation; k_a is the association rate constant for the two monomers forming dimer; k_d is the equivalent of the dissociation rate constant at the coalescence temperature T_c, which is the coalescence temperature for two signals derived from two different species in equilibrium with one another that coalesce; and $\Delta\nu$ is the peak separation in Hz. From K_a and k_d, k_a at the coalescence temperature was calculated, from which were calculated $\Delta G^{\ddagger}$ at T_c for both association and dissociation. Table VII records the results.

$$D \underset{k_a}{\overset{k_d}{\rightleftharpoons}} 2M \tag{15}$$

$$(K_a = k_a/k_d)_c \tag{16}$$

$$\Delta G^{\ddagger} = 4.57T_c\{10.32 - \log(k_c/T_c)\} \text{ in cal mol}^{-1} \tag{17}$$

Dimers in the Gas Phase. Dalcanale[21] has reported complex-

(18) Smithrud, D. B.; Diederich, F. J. *J. Am. Chem. Soc.* **1990**, *112*, 339–343.

(19) For the definition of E_T (30) values of solvents, see: (a) Langhals, H. *Angew. Chem., Int. Ed. Engl.* **1982**, *21*, 724–733. (b) Reichardt, C.; Dimroth, K. *Top Curr. Chem.* **1968**, *11*, 1–73. (c) Reichardt, C. *Solvents and Solvent Effects in Organic Chemistry*, 2nd ed.; VCH: Weinheim, 1988; Chapter 7, pp 339–405.

(20) Sandstrom, J. *Dynamic NMR Spectroscopy*; Academic Press: New York, 1982; pp 77–123.

(21) Dalcanale, E.; Soncini, P.; Bacchilega, G.; Ugozzoli, F. *J. Chem. Soc., Chem. Commun.* **1989**, 500–502.

(22) Bondi, A. *J. Phys. Chem.* **1964**, *68*, 441–451.

Table IX. Isotope Patterns for Velcraplexes ImidePz·ImidePz and UreaBz·UreaBz

ImidePz·ImidePz			UreaBz·UreaBz		
	%			%	
m/e	theory	obsd	m/e	theory	obsd
2921	53	32	2913	47	27
2922	100	93	2914	96	93
2923	97	100	2915	100	100
2924	65	63	2916	70	77
2925	33	50	2917	38	66
2926	14	22	2918	16	60
2927	5	12	2919	6	27
2928	2	7	2920	2	50

ation of neutral guests with an analogue of vase-shaped cavitand **3a** in the gas phase, the caviplex being detected by desorption chemical ionization mass spectrometry.

In the present study, we observed dimer peaks in the FAB MS obtained with a 3-nitrobenzyl alcohol (NOBA) matrix. The dimer peak was present in the spectra of only the more strongly bound homodimers in solution (MePz, ImidePz, UreaBz, ClPz, HQx, MeQx and ClQx) but was absent in the nonbound or weakly bound homodimers in solution (FPz, HPz, EtPz, CNPz, MeOPz and BrQx). Although the *dimer peaks when present* were weak compared to those of monomer, the data of Table VIII indicate a crude correlation between the relative abundance of dimer vs monomer in the gas phase and the $-\Delta G°$ values in $CDCl_3$. With the exception of BrQx, dimers with a $-\Delta G°$ value of greater than 4 kcal mol^{-1} give dimer signals. Table IX shows a good correlation between the observed and calculated isotope patterns for the peaks in the MS for the dimers of ImidePz and UreaBz.

Discussion

Velcraplex Structures. Chart III provides both top and side views of homodimers HPz·HPz, CH_3Pz·CH_3Pz, ClPz·ClPz, HQx·HQx, FMeNPz·FMeNPz, and monomer **2**. Examination of these six structures suggests the following conclusions. (1) Four aryl-attached methyl groups are inserted into four cavities complementary to the methyls in a lock-key arrangement which prevents rotation or slipping of one complexing partner with respect to the second (see A + B → C). (2) Substitution of the four $ArCH_3$ groups of **1** by the four ArEt groups of **2** gives a crystal of monomer whose core structure is conformationally identical (except for Et vs Me) to any *one* of the complexing partners in the five dimers. Thus, as suggested by CPK molecular examination, the monomers are preorganized for complexation. (3) A third feature common to the five dimer crystal structures is that four aryls of one partner are roughly in face-to-face contact with the four aryls of the second partner. This relationship is best visualized by the ball and stick face view of the crystal structure of HQx·HQx in Figure 1. (4) In all five structures, four pairs of peripheral aryl substituents are close (pseudo-gem) to one another, and four other pairs are distant (pseudo-meta) to one another. For example, in ClPz·ClPz (**4**), four pairs of chlorines are close and four pairs are distant. Four sets of Ar-X dipoles of one complexing partner are roughly aligned with four sets of Ar-X dipoles of the second complexing partner. (5) If the peripheral substituents are different as in FMeNPz·FMeNPz (**19·19**) several isomeric complexes might have formed, although only the one with the MeNH substituents close and the F substituents distant was observed (see top view of **19·19**). This dominance probably reflects the more stable structure for monomer in which each $NHCH_3$ group can sterically approach coplanarity with its attached aryl, and thus provide for stabilizing delocalization of charge symbolized by structure D. Moreover, four sets of Ar-F

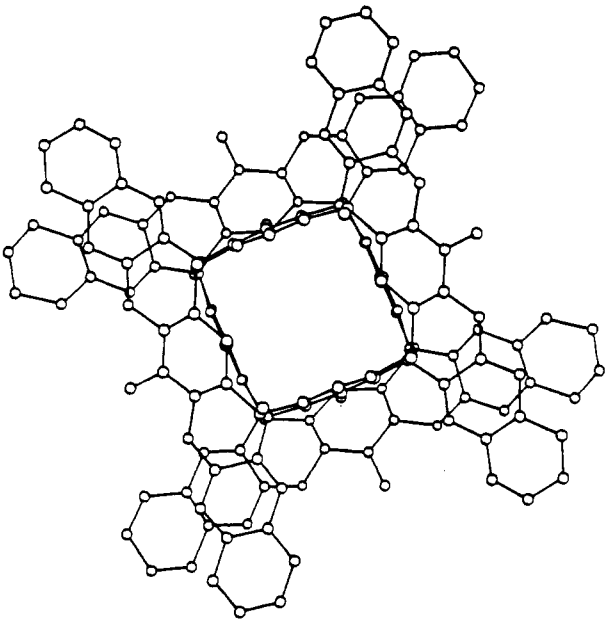

Figure 1. Ball and stick face-view of HQx·HQx Crystal Structure.

aligned dipoles are avoided in the conformation adopted by **19·19**. (6) If the differences in the conformations and disorder in the pentyl feet are disregarded, all of the velcraplexes possess only

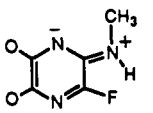

D

one approximate S_4 and two approximate mirror planes.

General Correlation of Complexation Free Energies with Structure. Table X contains the standard free energies ($-\Delta G°$) for homo- and heterodimerization calculated from the association constants of Tables I and II in the supplementary material. In all cases except the few indicated in the footnotes, $CDCl_3$ was solvent and 273 K, the temperature.

The most remarkable feature of the $-\Delta G°$ values is the range from <1 to >9 kcal mol^{-1}, depending on the peripheral substituents. The high values for binding in the absence of hydrogen bonding, metal ligating, ion-pairing, or hydrophobic effects is without parallel. This leaves dipole–dipole, van der Waals attractions, and solvophobic effects (other than hydrophobic) as the driving forces for complexation. We attribute the unusually high binding values to the unusually large surfaces shared by the binding partners and to the high degree of preorganization for binding of each monomer. The large preorganized and complementary shape of each monomer provides the potential for a large number of small but simultaneously acting attractive forces to be generated by dimerization. Thus, if a large number of small effects are additive, together they can produce large binding free energies.

The numbers of short intermolecular atomic distances listed in Table I taken from the crystal structures correlate roughly with the magnitudes of the $-\Delta G°$ values (Table X) for the four homodimers measured in $CDCl_3$ at 273 K. Obviously, the contributions of each kind of short contact vary widely. However, it is

dimer	no. of close contacts	$-\Delta G°$ (kcal mol^{-1}) total	$-\Delta G°$ (kcal mol^{-1}) av per contact
HQx·HQx	132	6.81	0.052
MePz·MePz	107	5.06	0.047
ClPz·ClPz	86	4.06	0.047
HPz·HPz	84	2.02	0.024

instructive to list the average contribution to the free energy of

(23) (a) Cram, D. J.; Stewart, K. D.; Goldberg, I.; Trueblood, K. N. *J. Am. Chem. Soc.* **1985**, *107*, 2574–2575. (b) Tucker, J. A.; Knobler, C. B.; Trueblood, K. N.; Cram, D. J. *J. Am. Chem. Soc.* **1989**, *111*, 3688–3699. (c) Conceill, J.; Lacombe, L.; Collet, A. *J. Am. Chem. Soc.* **1986**, *108*, 4230–4232.
(24) Van Geet, A. L. *Anal. Chem.* **1970**, *40*, 679–680.

Table X. Thermodynamic Parameters for Complexation at 273 K in $CDCl_3$

velcraplex	$-\Delta G°$ (kcal mol^{-1})	ΔH (kcal mol^{-1})	ΔS (cal mol^{-1} K^{-1})	correl factor[a]
HPz·HPz[b]	2.22[c]	−1.95	1.0	0.9947
HPz·MePz	4.60			
HPz·ClPz	4.41			
HPz·HQx	5.02			
HPz·MeQx[d]	>7.9			
HPz·ClQx[d]	>8.0			
MePz·MePz	5.06	−4.51	2.0	0.9760
FPz·MePz	5.36	−4.21	4.2	0.9946
MePz·ClPz[d]	>7.8			
MePz·HQx[d]	>8.9			
MePz·MeQx	8.88			
MePz·ClQx	7.39	−7.63	−0.4	0.9898
EtPz·EtPz[e]	<1.0			
FPz·EtPz[c]	2.32	−3.82	−5.5	0.9603
ClPz·EtPz[c]	3.76	−4.69	−3.4	0.9243
EtPz·CNPz[c]	2.50	−1.67	3.0	0.9869
CNPz·CNPz[f]	<1.0			
MeOPz·MeOPz[g]	<1.0			
MeOPz·ClPz[c]	2.51	−2.48	0.1	0.8533
MeOPz·FPz[f]	<1.0			
FPz·FPz[h]	<1.0			
ClPz·ClPz[c]	4.06	−3.76	1.1	0.9989
ClPz·HQx	6.69	−7.21	−1.9	0.9901
ClPz·MeQX[d]	>8.3			
ClPz·ClQx	5.66	−6.84	−4.2	0.9997
ClPz·FPz[f]	<1.0			
HQx·HQx	6.81	−7.28	−1.9	0.9632
HQx·MeQx	7.65	−6.78	3.0	0.9965
HQx·ClQx	8.03	−7.20	3.0	0.9999
MeQx·MeQx	6.20	−5.76	1.6	0.9846
MeQx·ClQx[d]	>9.2			
ClQx·ClQx	6.28	−6.08	0.5	0.9808
BrQx·BrQx	5.60	−4.98	2.3	0.9998
$NO_2Bz·NO_2Bz$[i]	<1.0			
$NO_2Bz·MePz$[c]	4.70	1.47	22.6	−0.9856
ImidePz·ImidePz[c]	5.63	5.35	40.4	−0.9954
ImidePz·HQx[j]	>9.1			
ImidePz·UreaBz[k]	<1.0			
UreaBz·UreaBz[l]	>9.0[m]			
$(HO)_2Qx·(HO)_2Qx$[n]	>8.1[o]			

[a] Correlation factor in van't Hoff plot. [b] CD_2Cl_2. [c] Extrapolated to 273 K. [d] 293 K. [e] 10 mM in CD_2Cl_2 at 183 K. [f] 10 mM at 223 K. [g] 20 mM in $CDCl_3$–$(CD_3)_2CO$ (1:1, v/v) at 203 K. [h] 50 mM in CD_2Cl_2 at 183 K. [i] 0.5 mM, 293–233 K. [j] If [ImidePz·HQx] >0.95 $[M]_t$, $-\Delta G° > 9.9$ kcal mol^{-1}. [k] 0.5 mM each at 313 to 333 K, only ImidePz·ImidePz and UreaBz·UreaBz were detected. The former gave $-\Delta G° = 5.55$ kcal mol^{-1}, $\Delta H = 6.00$ kcal mol^{-1}, $\Delta S = 42.3$ cal mol^{-1} K^{-1} ($R = 0.9940$). [l] Only dimer observed at 0.01 mM from 313 to 233 K and at 0.5 mM from 323 to 233 K. [m] If [D]/[M] > 9 at 273 K. If [D]/[M] > 4.5, then $-\Delta G° > 8.3$ kcal mol^{-1}. [n] Only dimer observed at 0.05 mM from 313 to 223 K. [o] If 5% monomer could have been observed; if 10% could have been observed, then $-\Delta G° > 7.4$ kcal mol^{-1}.

each contact. The values turned out to be remarkably close together: HQx·HQx, 0.052 (0.055) kcal mol^{-1}; MePz·MePz, 0.047 (0.042); ClPz·ClPz, 0.047 (0.044); and HPz·HPz, 0.024 (0.023) kcal mol^{-1}. The corresponding average enthalpies are listed parenthetically and provide a little wider spread, from 0.055 to 0.023 kcal mol^{-1} for each average contact. These average values involve much cancellation of various effects, particularly since they involve both the crystalline and liquid phases.

In each of these dimers, the eight locked methyl groups make contact[22] with many atoms of the corresponding guest molecule. Methyl carbon atoms contact 6–9 hydrogen atoms of the guest methyl group at distances of less than 3.2 Å. Methyl hydrogen–methyl hydrogen contacts (<2.7 Å) range from 2 in FMeNPz·FMeNPz to 8 in HQx·HQx. Methyl group–aryl group contacts are also important, ranging from 8 for HPz·HPz to 14 for HQx·HQx. The number of methyl group–oxygen contacts is nearly constant: C–O contacts range from 6 (HPz·HPz) to 10 (FMeNPz·FMeNPz), and H–O contacts range from 10 to 12. Methyl group to pyrazine group distances vary from dimer to dimer. Fewer contacts are found for HPz·HPz and FMeNPz·FMeNPz (4–6 contacts), and the most are found for HQx·HQx (14 contacts). Pyrazine (or quinoxaline) contacts are clearly important in all of these dimers. Although the types of short contacts vary, all of the dimers have 5–14 short C–N contacts (least for ClPz·ClPz and the most for FMeNPz·FMeNPz). All have 8–20 short C–C contacts (least for HPz·HPz and most for FMeNPz·FMeNPz). C–H, N–H, and H–H contacts are also important in HPz·HPz and MePz·MePz, N–Cl, O–Cl, and C–Cl contacts are important in ClPz·ClPz, and N–F and N–H contacts are important in FMeNPz·FMeNPz. Hydrogen atoms in all of these crystal structures are in calculated positions; these parameters have not been refined. However, the numbers of short contacts not involving hydrogen are quite significant in all five dimers.

All five of these dimers are very similar in their interplanar relationships involving pairs of pyrazine or quinoxaline groups. In every case the interplanar angles for the four group pairs in each dimer never exceed 6°; e.g., the pyrazine or quinoxaline groups are nearly parallel to each other at a distance of approximately 3.5 Å in each dimer.

Nondetectable Binding between Nonpreorganized Monomers. The importance of preorganization to binding is indicated by the fact that none of the pyrazine or benzene monomeric systems containing potentially noncoplanar substituents gave detectable homodimers (see Table X). Homodimers were not observed for EtPz, MeOPz, MeSPz, Me_2NPz, or NO_2Bz. In all of these systems, the four pairs of ortho substituents sterically inhibit each other from occupying conformations coplanar with their attached aryl rings. This effect is large enough in the Me_2NPz or MeSPz systems to inhibit heterodimerization as well but not great enough to disallow heterodimerization of EtPz, MeOPz, or NO_2Bz with partners containing coplanar substituents.

Coplanarity of the four pairs of ortho substituents did not guarantee that homodimerization would occur. Thus FPz and CNPz did not homodimerize, probably because of the four sets of aligned $Ar^{\delta+}$–$X^{\delta-}$ dipoles that would be found in their homodimers.

Coplanar Substituent Effects on Binding Free Energies of Homodimers. Table X provides the following decreasing order of $-\Delta G°$ values in kcal mol^{-1} for formation of the various homodimers that were studied in $CDCl_3$ at 273 K: UreaBz·UreaBz > 9.0; $(HO)_2Qx·(HO)_2Qx$, > 8.1; ClQx·ClQx, 6.8; HQx·HQx, 6.8; $CH_3Qx·CH_3Qx$, 6.2; BrQx·BrQx, 5.6; ImidePz·ImidePz, 5.6; MePz·MePz, 5.1; ClPz·ClPz, 4.1; HPz·HPz, 2.0; EtPz·EtPz, CNPz·CNPz, FPz·FPz, MeOPz·MeOPz, $NO_2Bz·NO_2Bz$, < 1.0. The order appears to be governed by a mixture of effects. CPK molecular model examination of UreaBz·UreaBz suggests that the most intermolecular proximate dipoles associated with the cyclic urea groups are largely compensating, which should enhance binding. This combined with solvophobic forces that favor binding might provide a system in which ΔH and $T\Delta S$ contributions to $\Delta G°$ are both negative and additive (see later section on enthalpy and entropy parameters). Similar CPK model examination of the syn isomeric dimer of $(HO)_2Qx·(HO)_2Qx$ indicates that it possesses a geometry very favorable for the existence of intermolecular hydrogen bonding of hydroxyl to hydroxyl and of hydroxyl to ether oxygens. Such attractive forces combined with the other contact attractions account for the >8.1 kcal mol^{-1} value for $-\Delta G°$. All of the $-\Delta G°$ values for the homodimers of the quinoxaline type are higher than any of the pyrazine or benzene types (an exception is that BrQx·BrQx and ImidePz·ImidePz both have $-\Delta G° = 5.6$ kcal mol^{-1}). We attribute this to the larger number of attractive contacts in the surfaces common to the complexing partners in the quinoxaline dimers as compared to the others (see former section).

Comparisons of Hetero- with Homodimerizations. An examination of Table X provides the generalization that with one important exception, heterodimers are more strongly bound than the corresponding more weakly-binding homodimer and frequently more than either of the corresponding two homodimers. Seven examples of the former and 15 of the latter are listed. We interpret this effect as reflecting the presence in all homodimers of four aligned pairs of proximate and identical dipoles. In the heterodimers, these aligned dipoles differ enough from one another to favor binding in some cases or to be less unfavorable to binding in others. The exception involves ImidePz and UreaBz, *which only homodimerize in the presence of one another.* That case will be discussed in a later section. A few examples are found in which a system incapable of homodimerizing can be induced to heterodimerize when mixed with one that does homodimerize.

Thus MeOPz and EtPz, which do not detectably homodimerize, respectively, form MeOPz·ClPz ($-\Delta G°$ = 2.5 kcal mol^{-1}) and EtPz·ClPz (3.8 kcal mol^{-1}) when mixed with ClPz, which does homodimerize. Similarly, NO_2Bz, which does not homodimerize, forms NO_2Bz·MePz (4.7 kcal mol^{-1}) when mixed with MePz, which does homodimerize. More striking are the heterodimers that are formed from two monomers, neither of which homodimerizes detectably. Examples are EtPz·FPz (2.3 kcal mol^{-1}) and EtPz·CNPz (2.5 kcal mol^{-1}).

Comparative Strengths of Binding in Heterodimers. Arrangement of the heterodimers of Table X in decreasing order of their binding strengths ($-\Delta G°$, kcal mol^{-1}) provides the following: MeQx·ClQx (>9.2); ImidePz·HQx (>9.1); MePz·HQx (>8.9); MePz·MeQx (8.9); ClPz·MeQx (>8.3); HPz·ClQx (>8.0); HQx·ClQx (8.0); HPz·MeQx (>7.9); MePz·ClPz (>7.8); HQx·MeQx (7.7); MePz·ClQx (7.4); ClPz·HQx (6.7); ClPz·ClQx (5.6); MePz·FPz (5.4); HPz·HQx (5.0); NO_2Bz·MePz (4.7); HPz·MePz (4.6); HPz·ClPz (4.4); EtPz·ClPz (3.8); MeOPz·ClPz (2.5); EtPz·CNPz (2.5); EtPz·FPz (2.3); ImidePz·UreaBz (<1.0); MeOPz·FPz (<1.0). Generally the heterodimers fall into three groups with respect to their stabilities. Those composed of two unlike quinoxalines, or one quinoxaline and a pyrazine, have $-\Delta G°$ values that range from 6.7 (ClPz·HQx) to >9.2 kcal mol^{-1} (MeQx·ClQx). Those heterodimers containing two pyrazines with electronically unlike but coplanar substituents provide $-\Delta G°$ values that run from 4.4 (HPz·ClPz) to >7.8 kcal mol^{-1} (MePz·ClPz). Those heterodimers containing two electronically similar pyrazines or a pyrazine and a benzene with one set of noncoplanar substituents provide $-\Delta G°$ values that range from <1.0 (e.g., MeOPz·FPz, ClPz·FPz) up to 4.7 kcal mol^{-1} (NO_2Pz·MePz). The three effects reflected in these three crude classes appear to be the numbers of close atom contacts between the two complexing partners, the electronic complementarity between the substituents, and the extent of preorganization of the substituents.

Enthalpies and Entropies of Complexation. The enthalpies and entropies of complexation listed in Table X in $CDCl_3$ as solvent show an *unparalleled spread of values with changes in structures of the complexing partners*. At one extreme of the ΔH values is −7.6 kcal mol^{-1} (ΔS is −0.4 cal mol^{-1} K^{-1}) for MePz·ClQx, signifying the complexing process is *enthalpy driven and entropy neutral*. At the opposite extreme of the ΔH values is +5.4 kcal mol^{-1} (ΔS is +40.4 cal mol^{-1} K^{-1}) for ImidePz·ImidePz, indicating a dimerization process which is *entropy driven* ($-T\Delta S$ is −11.0 kcal mol^{-1} at 273 K) and enthalpy opposed, giving a $\Delta G°$ value of −5.6 kcal mol^{-1}. Most host–guest complexations in nonhydroxylic media are *enthalpy driven* and *entropy opposed*, with ΔH values ranging from −3 to −8 kcal mol^{-1} and ΔS values from −12 to −18 cal mol^{-1} K^{-1}.

Formation of ImidePz·ImidePz provides one extreme for the entropy of complexation. The only other example in Table X of an entropy-driven process involves formation of NO_2Bz·MePz, whose entropy is 22.6 cal mol^{-1} K^{-1} to provide at 273 K, a $-T\Delta S$ value of −6.2 kcal mol^{-1} opposed by a +1.5 kcal mol^{-1} ΔH value. Thus, this dimerization is *entropy driven but enthalpy* weakly opposed. The most extreme example of a negative entropy is −5.5 cal mol^{-1} K^{-1} for the formation of EtPz·FPz. This dimerization provides a $-T\Delta S$ value at 273 K of +1.5 kcal mol^{-1}, while ΔH = −3.8 kcal mol^{-1} to give a $\Delta G°$ value of −2.3 kcal mol^{-1}, thus illustrating an *enthalpy driven* and *entropy opposed* process. The closest example to a *combined enthalpy and entropy driven* dimerization involves formation of MePz·FPz, whose ΔH is −4.2, ΔS is +4.2 ($-T\Delta S$ at 273 K is −1.1 kcal mol^{-1}), and $\Delta G°$ is −5.3 kcal mol^{-1}. Most of the other 14 dimers whose enthalpies and entropies are reported in Table X are *enthalpy driven* and *entropy neutral* (ΔS values vary from extremes of +3.0 to −4.2, but 9 are ±2 cal mol^{-1} K^{-1}). UreaBz·UreaBz is bound so strongly that monomer was never detected, but the large changes of [UreaBz·HQx] to [HQx·HQx] ratios compared to changes of [HQx·HQx] itself with changes in temperature in equal molar mixtures of the two systems strongly suggest that the formation of UreaBz·UreaBz is entropy driven. Thus all of the dimerizations studied possess entropies of formation that are either much less negative than usual or are positive, in some cases strongly positive, enough to be entropy driven.

We correlate these effects as follows. The binding surfaces of two monomers are large enough to be solvated by 16 to 18 molecules of $CDCl_3$, each molecule of which is weakly bound and somewhat oriented, depending on the polarity of the substituent groups that compose the surfaces. When dimerization occurs, these 16 to 18 molecules are detached from the surface and become ordinary randomly oriented solvent molecules. The desolvation process involves overcoming solvent-to-surface attractions (a positive enthalpy), but the liberation of many more or less oriented solvent molecules to solvent increases randomness (a positive entropy). With polar substituents such as the 16 nitro groups of $2NO_2Bz$, the 16 carbonyl groups of 2ImidePz, or the 16 N···C···O moieties of 2UreaBz, these effects outweigh the *negative enthalpies* of two monomers sharing a large common, rigid surface and the *negative entropies* of collecting and locking two monomers into a dimer. These same effects are present in all the dimerizations, but the enthalpic effects of solvent-to-surface attractions and accompanying entropic effects of solvent orientations are outweighed particularly by the monomer-to-monomer attractions in the dimer to make enthalpically driven, entropy neutral processes the most commonly encountered. In other words, "solvophobic" binding driving forces are present in all of these dimerizations, and sometimes they are dominant.

A few specific cases are particularly interesting and instructive. Notice that EtPz·FPz has the most negative entropy of formation (−5.5 cal mol^{-1} K^{-1}). Examination of a CPK model of this dimer shows that the conformational freedom of eight ethyl groups have to be limited in this dimerization, entailing an additional entropic cost. In the formation of MePz·FPz and NO_2Bz·MePz, both the enthalpy and entropy favor complexation by at least −1 kcal mol^{-1}, which is unusual. Even more unusual is the fact that although ImidePz and UreaBz form strongly bound homo- and heterodimers, they give no detectable ImidePz·UreaBz when mixed. We can only point to the complexities of the multiple dipoles in each system, which appear to be overall electronically nonfavorable for attractions in this mixed dimer or, at least, much less attracting than in the homodimer.

Solvent Effects on Binding Free Energies of Dimers. Table III lists the $-\Delta G°$ values for MePz·MePz formation in a variety of solvents, along with the solvents' polarizability parameters [E_T (30)]. For the seven solvents that allowed $-\Delta G°$ values to be measured, the values ranged from a low of 4.25 for CCl_4 to a high of 5.19 kcal mol^{-1} for $(CD_2)_4O$, covering a change from 32.4 to 40.7 in E_T (30) units. No correlation between $-\Delta G°$ and E_T (30) values is evident. The solvents were CCl_4, $C_6D_5CD_3$, C_6D_6, C_6D_5Cl, $(CD_2)_4O$, $CDCl_3$, and CD_2Cl_2. Furthermore, for both $(CD_2)_6$ and $(CD_3)_2CO$ whose respective E_T (30) values are 30.9 and 42.2, $-\Delta G°$ values are both >6.3 kcal mol^{-1}. Thus within this range of nine different solvents covering a spread in E_T (30) values of 11 units, the relationship between $-\Delta G°$ and E_T (30) is essentially random. In proceeding to more polar solvents such as $(CD_3)_2NCDO$, CD_3CN, CD_3NO_2, CD_3CD_2OD, and CD_3OD, only dimer was detected, indicating very high inaccessible values for $-\Delta G°$ in these solvents. We conclude that the linear free energy relationship of Diederich and Smithrud[18] can apply only in systems where the entropies of solvation of both host and guest remain relatively constant or vary in such a way as to remain proportional to ΔH.

Table IV reports the results of a second study of the effect of solvent on $-\Delta G°$ values, in this case involving the dimerization of ClPz. The $-\Delta G°$ values with $CDCl_3$, CD_2Cl_2, or $C_6D_5CD_3$ were essentially the same at ~4.1 kcal mol^{-1} and changed little with temperature. Solvents composed of $CDCl_3$ diluted with differing amounts (v/v) of $(CD_3)_2CO$, CD_3OD, and CD_3NO_2 were then added, and the $-\Delta G°$ values determined at −18 °C. By the time 25% of $(CD_3)_2CO$, CD_3NO_2, or CD_3OD had been added, $-\Delta G°$ values had reached 5.1, 5.3, and >5.6 kcal mol^{-1}, respectively. When 50% of $(CD_3)_2CO$ or 100% $(CD_3)_2CO$ were employed, $-\Delta G° > 5.9$ kcal mol^{-1}. Thus large increases in solvent polarizability induce large increases in the free energy of binding with

Table XI. Free Energies of Association in $CDCl_3$ at 273 K and Activation Free Energies for Association and Dissociation at Coalescence Temperatures (T_c)[a]

velcraplex	$-\Delta G°$ (kcal mol^{-1})	$\Delta G^{\ddagger}_a$ (kcal mol^{-1})	$\Delta G^{\ddagger}_d$ (kcal mol^{-1})	T_c (K)
FPz·MePz	5.4	10.0	15.5	315
ClPz·ClPz	4.1	9.95	14.0	285
ClPz·EtPz	3.8	9.6	13.3	273
FPz·EtPz	2.3	9.2	11.6	243
HPz·HPz[b]	2.0	8.1	10.1	213

[a] Taken from Tables X and VII. [b] CD_2Cl_2 as solvent.

this system, presumably reflecting increased solvophobic driving forces as the solvent becomes more polar. Table VII indicates that in $CDCl_3$, ΔH (kcal mol^{-1}) values range only between −3.8, −4.1, and −4.0 as the solvent was changed from $CDCl_3$ to 10% $(CD_3)_2CO$ to 10% CD_3OD in $CDCl_3$, respectively. The respective ΔS (cal mol^{-1} K^{-1}) values changed only from 1.1 to 2.0 to 2.8.

Table VI gives the results of solvent and temperature changes on the thermodynamic parameters for ImidePz, whose dimerization in $CDCl_3$ is *entropy driven* and *enthalpy opposed*. In CD_2Cl_2 at 273 K, $-\Delta G°$ = 5.5 kcal mol^{-1} (extrapolated value), ΔH = 5.8 kcal mol^{-1}, and ΔS = 33.7 cal mol^{-1} K^{-1}, which are values close to those in $CDCl_3$ at 273 K ($-\Delta G°$ = 5.6 kcal mol^{-1}, ΔH = 5.35 kcal mol^{-1}, and ΔS = 40.4 cal mol^{-1} K^{-1}). In CCl_4–CD_2Cl_2 (4/1, v) at 273 K (the CD_2Cl_2 was present for solubility reasons), $-\Delta G°$ = 7.0 kcal mol^{-1} (extrapolated value), ΔH = 2.34 kcal mol^{-1}, and ΔS = 37.8 cal mol^{-1} K^{-1}. Thus solvent changes from $CDCl_3$ to CD_2Cl_2 to CCl_4–CD_2Cl_2 (4/1, v) had little effect on this *entropy driven, enthalpy opposed* dimerization. In an attempt to use CD_2Cl_2–CD_3OD (1/1, v) as solvent, $-\Delta G°$ was only on scale at 193 K, and gave a value of $-\Delta G$ = 4.9 kcal mol^{-1}. At temperatures from 223 to 303 K, $-\Delta G$ > 6 kcal mol^{-1}. These results suggest that in this solvent as well the dimerization could be even more entropy driven.

Activation Free Energies for Association and Dissociation. Table XI records the free energies for association at 273 K and the activation free energies for association ($\Delta G^{\ddagger}_a$) and dissociation ($\Delta G^{\ddagger}_d$) at T_c involving two homodimerizations and three heterodimerizations in $CDCl_3$.

The five systems (MePz·FPz, ClPz·ClPz, EtPz·ClPz, EtPz·FPz, and HPz·HPz) are arranged in decreasing order of their $\Delta G°$, $\Delta G^{\ddagger}_a$, $\Delta G^{\ddagger}_d$, and T_c values, which all correlate to produce the same monotonic trend. The total spread in $-\Delta G°$ values is 3.4 kcal mol^{-1}, whereas that for $\Delta G^{\ddagger}_a$ is 1.9 and for $\Delta G^{\ddagger}_d$ is 5.4 kcal mol^{-1}. This suggests the transition state structure is closer to the dimers than to the monomers.

The activation free energies for both the associative and dissociative processes are remarkably high for dimers held together only by dipole–dipole, van der Waals, and solvophobic forces. We attribute these high values to the fact that dimer formation involves exchanging attractions between up to 18 molecules of solvent and two large monomeric faces for attractions between two faces with approximately 100 close contacts. The rigid preorganization of these surfaces make them nonadaptive to an incremental and simultaneous exchange of solvent-to-monomer attractions for monomer-to-monomer attractions. The four methyl-into-cavity locks when engaged prevent one partner from *slipping or rotating* with respect to the second partner until most of the close contacts have disappeared. The strong partner-to-partner or monomer attractions to solvent present in one or the other starting state are absent in the transition state, thus accounting for the 8 to 15 kcal mol^{-1} transition state energies. Were it not for the solvophobic effect of drowning most of the original solvating molecules in the bulk solvent by the time the transition state is reached from the monomer side, $\Delta G^{\ddagger}_a$ would be much higher.

Summary

Eighteen new velcrands possessing large rigid surfaces have been prepared, 16 of which hetero- or homodimerize in $CDCl_3$ at 273 K with binding free energies ($-\Delta G°$) that range from <1 to >9.2 kcal mol^{-1} depending on substituents attached to their peripheries. Crystal structures of five dimers show them to contain common surfaces composed of 82–132 atom-to-atom close contacts (≤van der Waals + 0.2 Å) between monomers, which are immobilized in the dimer by insertion of four protruding methyls into four cavities stereoelectronically complementary to the methyls. The binding forces are dipole–dipole, van der Waals, and solvophobic in character. With notable exceptions, binding free energies increase with solvent polarity, the size of the surface common to the two monomers in the dimers, and the stereoelectronic complementarity and conformational immobility of peripheral substituents. Examples of dimerizations were observed that were *entropy driven* (up to −11 kcal mol^{-1}) and enthalpy opposed (+5.5 kcal mol^{-1}), enthalpy driven (up to −7.2 kcal mol^{-1}), and *entropy opposed* (+0.6 kcal mol^{-1}), and *both enthalpy* (up to −7.2 kcal mol^{-1}) and *entropy driven* (−0.8 kcal mol^{-1}). Activation free energies for complexation in $CDCl_3$ varied from 8.1 to 10.0 kcal mol^{-1}, for decomplexation from 10.1 to 15.5 kcal mol^{-1}, and both increased monotonically with increases in $-\Delta G°$ values as substituents were varied. For the first time, a family of complexing partners has been studied which allowed solvophobic binding effects to be dominant or at least discernible in organic solvents as nonpolar as $CDCl_3$, CCl_4, CD_2Cl_2, and $(CD_2)_6$.

Experimental Section

General Methods. Before use, anhydrous 99% plus grade $(CH_3)_2NCOCH_3$ (DMA), $(CH_3)_2NCHO$ (DMF), $(CH_3)_2SO$ (DMSO), or 1,4-dioxane were transferred with double-tipped needles and degassed under high vacuum. THF ($(CH_2)_4O$) was distilled from benzophenone ketyl immediately prior to use. Anhydrous CH_2Cl_2 was obtained either by distilling from CaH_2 or by passing through a column packed with super activity I neutral alumina. Pyridine was dried over KOH, distilled from BaO, and stored over 4 Å molecular sieves. Samples were dried in a pistol at 110 °C for 24 h prior to elemental analyses. All ^{1}H NMR spectra were obtained on Bruker AF 200, AM 360, or AM 500 spectrometers. All chemical shifts were measured either relative to TMS (δ = 0.00) or residual solvent resonances (δ $CHCl_3$ = 7.26, δ DMSO = 2.49, δ CD_3CN = 1.93, δ CD_2Cl_2 = 5.32 ppm). All ^{13}C NMR spectra were obtained on the AM 360 instrument at 90 MHz. Chemical shifts were measured relative to solvent ^{13}C resonances (δ $CDCl_3$ = 77.00, δ CD_3CN = 1.3 or 118.2, δ CD_2Cl_2 = 53.8 ppm). Melting points for high melting samples over 250 °C were determined on a Mel-Temp apparatus, and for low melting samples below 250 °C on a Thomas-Hoover apparatus, and are uncorrected. Analytical thin layer chromatography (TLC) was performed using Merck DC-Fertigplatten Kieselgel 60 F-254 (20 × 20 cm) 0.25 mm silica gel precoated glass plates, Merck DC-Plastikfolien Aluminiumoxid 60 F_{254} neutral (type E) (20 × 20 cm) 0.2 mm plastic sheets, or Whatman Reversed Phase $KC_{18}F$ (20 × 20 cm) 200 μL octadesylsilane bonded precoated glass plates. Spots were visualized under UV light. Column chromatography at elevated pressure (flash) was performed using EM Science silica gel 60 (particle size 0.040–0.063 mm, 230–400 mesh ASTM). Filtration column chromatography utilized EM Science silica gel 60 (particle size 0.063–0.200 mm, 70–230 mesh ASTM). All reactions were carried out under a slightly positive pressure of dry argon with magnetic stirring unless otherwise indicated. All glassware used was either oven dried for >2 h at >120 °C or flame dried under vacuum.

Known Bridging Compounds. Syntheses and identifications of **22**, **26–29**, and **31** are found in the supplementary material.

5,6-Dichloropyrazine-2,3-dicarboxylic Acid. To 800 mL of vigorously boiling water was added 10 g of 2,3-dichloroquinoxaline and then 53 g of $KMnO_4$ in portions over 30 min. The mixture was further heated at 95–98 °C for 2 h. The solid MnO_2 was removed by filtration from the hot suspension. The solid MnO_2 was boiled with 100 mL of water and filtered, and this procedure was repeated. The warm combined aqueous filtrate was acidified with 33 mL of concentrated aqueous HCl. The acidic filtrate was concentrated by rotary evaporator, and the residue was completely dried in vacuo. The solid residue was extracted with two 150-mL portions of acetone. The filtrate was concentrated and dried in vacuo to afford 5.85 g (49%) of product, which was recrystallized from acetone: mp >220 °C (dec); ^{13}C NMR (50 MHz, $(CD_3)_2CO$) δ 163.96, 148.42, 143.32; MS, *m/e* 236 (M^+, 1.8%). Anal. Calcd for $C_6H_2N_2O_4Cl_2$: C, 30.41; H, 0.85; N, 11.82. Found: C, 30.49; H, 1.06; N, 11.61.

5,6-Dichloropyrazine-2,3-dicarboxylic Acid Anhydride. A mixture of 5,6-dichloropyrazine-2,3-dicarboxylic acid (2.3 g) in 5 mL of $SOCl_2$ was refluxed for 30 min. The excess $SOCl_2$ was evaporated, and the crystalline residue was dried in vacuo. The residue was dissolved in 50 mL of EtOAc and decolorized with charcoal. After removing the charcoal

by filtration, the filtrate gave upon standing 1.32 g (62%) of product: mp 250–252 °C; ^{13}C NMR (90 MHz, $(CD_3)_2CO$) δ 158.18, 155.42, 143.98; MS, 218 (M^+, 23%). Anal. Calcd for $C_6N_2O_3Cl_2$: C, 32.91; H, 0.0; N, 12.79. Found: C, 32.78; H, trace; N, 12.81.

5,6-Dichloropyrazine-2,3-dicarboxylic Acid Methylimide (30). A mixture of 5,6-dichloropyrazine-2,3-dicarboxylic acid anhydride (0.438 g) and CH_3NH_3Cl (0.24 g) in 0.5 mL of Ac_2O was heated in a closed flask at 120 °C for 20 min. The cooled crystalline reaction mixture was washed with water and dried in vacuo to yield 0.435 g (94%) of white crystalline product: mp 242–244 °C; ^{1}H NMR (360 MHz, $CDCl_3$) δ 3.32 (s); ^{13}C NMR (90 MHz, $CDCl_3$) δ 162.16, 153.49, 143.70, 24.78; MS *m/e* 231 (M^+, 36.5%). Anal. Calcd for $C_7H_3N_3O_2Cl_2$: C, 36.24; H, 1.30; N, 18.11. Found: C, 36.59; H, 1.44; N, 17.84.

Pentacyclo[19,3,1,1^{3,7},1^{9,13},1^{15,19}]octacosa-1(25),3,5,7(28),9,11,13-(27),15,17,19(26),21,23-dodecaene-4,6,10,12,16,18,22,24-octol, 2,8,14,20-Tetrapentyl-5,11,17,13-tetramethyl-, Stereoisomer (Octol, 33). Hexanal (100 g, 1 mol) and 2-methylresorcinol (124 g, 1 mol) were dissolved in 500 mL of absolute ethanol, and to this solution were added 500 mL of water and 250 mL of concentrated HCl. The solution was mechanically stirred at 80 °C. The sticky yellow precipitate formed after 1 h slowly becomes an amorphous solid. The reaction mixture was stirred for 4 days at 80 °C and was cooled to 25 °C. The solid precipitate was obtained by filtration. The crude product was triturated with water and filtered, and this process was repeated until the residual acid was completely removed. The solid product was dried in air and in vacuo to yield 168 g (81%) of a slightly yellow solid. This product was pure enough for the next step but was recrystallized from acetone or methanol: mp >260 °C dec; ^{1}H NMR (360 MHz, $(CD_3)_2SO$) δ 8.67 (s, 8 H, -OH), 7.25 (s, 4 H, ArH), 4.21 (t, *J* = 7.5 Hz, -CH), 2.21 (m, 8 H, -CH-CH_2-), 1.96 (s, 12 H, Ar-CH_3), 1.34–1.2 (m, 24 H, -$CH_2CH_2CH_2CH_3$), 0.86 (t, *J* = 7.5 Hz, 12 H, -CH_3); MS (FAB, NOBA) *m/e* 825 (M^+ + 1, 33%). Anal. Calcd for $C_{52}H_{72}O_8 0.5H_2O$: C, 74.88; H, 8.70. Found: C, 74.94; H, 8.68.

27,37:28,36-Dimetheno-29*H*,31*H*,33*H*,35*H*-pyrazino[2″,3″:2′,3′]-[1,4]benzodioxonino[10′,9′:5,6]pyrazino[2″,3″:2′,3′]pyrazino-[2‴,3‴:2‴,3‴][1,4]dioxonino[6‴,5‴:9′,10′][1,4]benzodioxonino-[6′,5′:9,10][1,4]benzodioxonino[2,3-*b*]pyrazine, 2,3,9,10,16,17,23,24-Octachloro-6,13,20,39-tetramethyl-29,31,33,35-tetrapentyl-, Stereoisomer (ClPz, 4). Procedure A. A mixture of octol **33** (1.65 g, 2 mmol), tetrachloropyrazine (**28**) (1.91 g, 8.8 mmol), and K_2CO_3 (4.0 g) in 150 mL of DMF was stirred at 25 °C for 24 h. The solvent was removed in vacuo, and the residue was partitioned between CH_2Cl_2 and water. The CH_2Cl_2 layer was separated, dried over $MgSO_4$, and concentrated in vacuo. The product was filtered through a short silica gel column eluting with CH_2Cl_2. The solid product (1.6 g, 57%) was obtained after evaporating the CH_2Cl_2. The product was recrystallized from acetone or nitrobenzene: mp >360 °C (dec); ^{1}H NMR (360 MHz, $CDCl_3$, 25 °C) δ 6.96 (s, 2 H, Ar-H), 6.04 (s, 2 H, Ar-H), 3.65 (m, 4 H, -CH-), 2.58 (s, 6 H, Ar-CH_3), 1.95 (m, 14 H, Ar-CH_3 and -CH-CH_2-), 1.22 (m, 24 H, -$CH_2CH_2CH_2$-CH_3), 0.83 (t, 12 H, -CH_3); dimer (360 MHz, $CDCl_3$, 255 K) δ 6.93 (s, 2 H, Ar-H), 6.02 (s, 2 H, Ar-H), 3.60 (m, 4 H, -CH-), 2.62 (s, 6 H, Ar-CH_3), 1.92 (m, 8 H, -CH-CH_2-), 1.69 (s, 6 H, Ar-CH_3); monomer (360 MHz, $CDCl_3$, 255 K) 7.03 (s, 2 H, Ar-H), 6.05 (s, 2 H, Ar-H), 3.70 (m, 4 H, -CH-), 2.48 (s, 6 H, Ar-CH_3), 2.19 (s, 6 H, Ar-CH_3), 2.01 (m, 8 H, -CH-CH_2-) (the -$CH_2CH_2CH_2$-CH_3 resonances of monomer and dimer overlap); MS (FAB, NOBA) *m/e* 1404 (M^+, 100%). Anal. Calcd for $C_{68}H_{64}Cl_8N_8O_8$: C, 58.13; H, 4.59. Found: C, 57.86; H, 4.71.

27,37:28,36-Dimetheno-29*H*,31*H*,33*H*,35*H*-pyrazino[2″,3″:2′,3′]-[1,4]benzodioxonino[10′,9′:5,6]pyrazino[2″,3″:2′,3′]pyrazino-[2‴,3‴:2‴,3‴][1,4]dioxonino[6‴,5‴:9′,10′][1,4]benzodioxonino-[6′,5′:9,10][1,4]benzodioxonino[2,3-*b*]pyrazine, 2,3,9,10,16,17,23,24-Octafluoro-6,13,20,39-tetramethyl-29,31,33,35-tetrapentyl-, Stereoisomer (FPz, 8). To a solution of tetrafluoropyrazine (2.78 g, 18 mmol) in 350 mL of DMF was added dropwise a mixture of octol **33** (3.3 g, 4 mmol) and K_2CO_3 (3.3 g) in 150 mL of DMF at 25 °C. The mixture was stirred for 18 h at 25 °C and then treated as in procedure A. The white product obtained was triturated with hexane to give **8**, 1.856 g (36%): mp 324–326 °C; ^{1}H NMR (360 MHz, $CDCl_3$) δ 7.03 (s, 2 H, Ar-H), 6.05 (s, 2 H, Ar-H), 3.79 (m, 4 H, -CH-), 2.46 (s, 6 H, Ar-CH_3), 2.16 (s, 6 H, Ar-CH_3), 2.01 (m, 8 H, -CH-CH_2-), 1.28 (m, 24 H, -$CH_2CH_2CH_2$-CH_3), 0.86 (t, *J* = 7.0 Hz, 12 H, -CH_3); ^{13}C NMR (90 MHz, $CDCl_3$) δ 151.5, 149.7, 144.4 (br), 140.1, 138.1, 134.7, 132.8, 127.3, 122.8, 119.5, 118.3, 37.5, 31.9, 31.7, 26.6, 22.4, 14.0, 11.1, 10.9; ^{19}F NMR (339 MHz, $CDCl_3$, $CFCl_3$ referenced as 0) δ −71.65 (d, *J* = 19.2 Hz), −75.61 (d, *J* = 19.2 Hz); MS (FAB, NOBA) *m/e* 1272 (M^+, 100%). Anal. Calcd for $C_{68}H_{64}F_8N_8O_8$: C, 64.14; H, 5.07; N, 8.80. Found: C, 64.05; H, 5.03; N, 8.73.

27,37:28,36-Dimetheno-29*H*,31*H*,33*H*,35*H*-pyrazino[2″,3″:2′,3′]-[1,4]benzodioxonino[10′,9′:5,6]pyrazino[2″,3″:2′,3′]pyrazino-[2‴,3‴:2‴,3‴][1,4]dioxonino[6‴,5‴:9′,10′][1,4]benzodioxonino-[6′,5′:9,10][1,4]benzodioxonino[2,3-*b*]pyrazine, 6,13,20,39-Tetramethyl-29,31,33,35-tetrapentyl-, Stereoisomer (HPz, 5) (Procedure B). A mixture of octol **33** (413 mg, 0.5 mmol), 2,3-dibromopyrazine **25** (525 mg, 2.2 mmol), CuO (800 mg, 10 mmol), and K_2CO_3 (690 mg, 5 mmol) in 10 mL of DMA was heated at 80 °C for 4 h and then at 140 °C for 4 h. The solvent was removed in vacuo. The residue was dissolved in CH_2Cl_2, and insoluble material was removed by filtration. The filtrate was washed with water, dried over $MgSO_4$, and concentrated in vacuo. The product was purified by column chromatography (silica gel, EtOAc–hexane (1:1)) to yield 285 mg (50%) of HPz, recrystallized from $(CH_3)_2CO$–CH_2Cl_2: mp 331–333 °C; ^{1}H NMR (500 MHz, $CDCl_3$, 60 mM), δ 8.05 (d, *J* = 2.4 Hz, 4 H, Pz-H), 7.82 (d, *J* = 2.4 Hz, 4 H, Pz-H), 6.98 (s, 2 H, Ar-H), 6.10 (s, 2 H, Ar-H), 3.67 (t, *J* = 7.5 Hz, 4 H, -CH-), 2.55 (s, 6 H, Ar-CH_3), 2.22 (s, 6 H, Ar-CH_3), 1.97 (m, 8 H, -CH-CH_2-), 1.25 (m, 24 H, -$CH_2CH_2CH_2$-CH_3), 0.83 (t, *J* = 7.0 Hz, 12 H, -CH_3); ^{13}C NMR (90 MHz, $CDCl_3$) δ 151.8, 151.4, 150.4, 146.7, 138.7, 136.3, 134.3, 131.4, 127.8, 122.8, 118.9, 117.7, 37.6, 31.8, 26.6, 22.3, 14.0, 11.5, 11.2; MS (FAB) *m/e* 1130 (M^+ + 2, 61.9%), *m/e* 1129 (M^+ + 1, 100%), *m/e* 1128 (M^+, 55.1%), *m/e* 1127 (25.0%), *m/e* 1157 (M^- C_5H_{11}, 6.1%). Anal. Calcd for $C_{68}H_{72}N_8O_8$: C, 72.32; H, 6.43; N, 9.92. Found: C, 72.38; H, 6.54; N, 9.82.

27,37:28,36-Dimetheno-29*H*,31*H*,33*H*,35*H*-pyrazino[2″,3″:2′,3′]-[1,4]benzodioxonino[10′,9′:5,6][pyrazino[2″,3″:2′,3′]pyrazino-[2‴,3‴:2‴,3‴][1,4]dioxonino[6‴,5‴:9′,10′][1,4]benzodioxonino-[6′,5′:9,10][1,4]benzodioxonino[2,3-*b*]pyrazine, 2,3,6,9,10,13,16,17,20,-23,24,39-Dodecamethyl-29,31,33,35-tetrapentyl-, Stereoisomer (MePz, 6). A mixture of octol **33** (413 mg, 0.5 mmol), 2,3-dibromo-5,6-dimethylpyrazine (**26**) (585 mg, 2.2 mmol), CuO (800 mg, 10 mmol), and K_2CO_3 (690 mg, 5 mmol) in 10 mL of DMA was heated at 90 °C for 5 h and then at 140 °C for an additional 3 h. The product was isolated as in procedure B, except that EtOAc–hexane (3:7, v) eluted **6** from silica gel, and the material was rechromatographed on alumina–CH_2Cl_2 to give 375 mg (60%) of MePz: mp > 360 °C (dec); ^{1}H NMR (500 MHz, $CDCl_3$, 20 mM, 20 °C) δ 6.83 (s, 2 H, Ar-H), 6.04 (s, 2 H, Ar-H), 3.63 (m, 4 H, -CH-), 2.67 (s, 6 H, Ar-CH_3), 2.39 (s, 12 H, Pz-CH_3), 2.22 (2, 12 H, Pz-CH_3), 1.86 (br s, 14 H, Ar-CH_3 and -CH-CH_2-), 1.13 (m, 24 H, -$CH_2CH_2CH_2CH_3$), 0.76 (t, 12 H, -CH_3); dimer (500 MHz, $CDCl_3$, 1 mM −20 °C) δ 6.83 (s, 2 H, Ar-H), 6.01 (s, 2 H, Ar-H), 3.60 (m, 4 H, -CH-), 2.69 (s, 6 H, Ar-CH_3), 2.39 (s, 12 H, Pz-CH_3), 2.22 (s, 12 H, Pz-CH_3), 1.83 (s, 6 H, Ar-CH_3), 1.78 (s, 8 H, -CH-CH_2-), 1.10 (m, 24 H, -$CH_2CH_2CH_2CH_3$), 0.75 (t, 12 H, -CH_3); monomer (500 MHz, $CDCl_3$, 1 mM, −20 °C) δ 6.98 (s, 2 H, Ar-H), 6.05 (s, 2 H, Ar-H), 3.77 (m, 4 H, -CH-), 2.50 (s, 18 H, Ar-CH_3 and Pz-CH_3), 2.36 (s, 12 H, Pz-CH_3), 2.28 (s, 6 H, Ar-CH_3), 1.87 (s, 8 H, -CH-CH_2-), 1.24 (m, 24 H, -$CH_2CH_2CH_2CH_3$), 0.83 (t, 12 H, -CH_3); ^{13}C NMR (90 MHz, $CDCl_3$ as dimer) δ 151.7, 150.2, 148.4, 143.3, 143.2, 133.7, 128.0 (br), 122.4, 118.4, 118 (br), 37.0, 32.0, 31.6, 26.6, 22.3, 20.8, 20.3, 14.0, 11.7, 11.4; MS (FAB, NOBA) *m/e* 1240 (M^+, 30%). Anal. Calcd for $C_{76}H_{88}N_8O_8$: C, 73.52; H, 7.14; N, 9.02. Found: C, 73.27; H, 6.93; N, 8.86.

6,16:7,15-Dimetheno-1*H*,8*H*,10*H*,12*H*,14*H*,19*H*,27*H*,35*H*-pyrrolo[3,4-*b*]pyrrolo[3‴,4‴:5″,6″]pyrazino[2″,3″:2′,3′][1,4]benzodioxonino[10′,9′:5,6]pyrrolo[3‴,4‴:5″,6″]pyrazino[2″,3″:2′,3′]pyrrolo-[3⁗,4⁗:5‴,6⁗]pyrazino[2⁗,3⁗:2⁗,3⁗][1,4]dioxonino-[6⁗,5⁗:9′,10′][1,4]benzodioxonino[6′,5′:9,10][1,4]benzodioxonino[2,3-*e*]pyrazine-1,3,19,21,27,29,35,37(2*H*,20*H*,28*H*,36*H*)-octone, 2,20,24,28,32,36,40,43-Octamethyl-8,10,12,14-tetrapentyl- (ImidePz, 16). To a solution of octol **33** (83 mg, 0.1 mmol) and imide **31** (112 mg, 0.48 mmol) in 4 mL of DMF was added 125 μL of Et_3N by syringe. The solution was heated at 80 °C for 5 h. The product was isolated as in procedure A to give 83 mg (57%) of ImidePz: ^{1}H NMR (360 MHz, $CDCl_3$, 25 °C) of dimer; δ 6.93 (s, 2 H, Ar-H), 6.08 (s, 2 H, Ar-H), 3.45 (m, 4 H, -CH-), 3.30 (s, 12 H, N-CH_3), 2.99 (s, 6 H, Ar-CH_3), 1.96 (s, 6 H, Ar-CH_3), 1.9 (br m, 8 H, -CH-CH_2-), 1.15 (br m, 24 H, -$CH_2CH_2CH_2$-CH_3), 0.77 (t, 12 H, CH_3); of monomer (1 mM, −30 °C) δ 7.00 (s, 2 H, Ar-H), 6.12 (s, 2 H, Ar-H), 3.58 (m, 4 H, -CH-), 3.24 (s, 12 H, N-CH_3), 2.51 (s, 6 H, Ar-CH_3), 2.32 (s, 6 H, Ar-CH_3), 1.9 (br m, 8 H, -CH-CH_2-), 1.15 (br m, 24 H, -$CH_2CH_2CH_2$-CH_3), 0.81 (t, 12 H, -CH_3); ^{13}C NMR (90 MHz, $CDCl_3$) δ 162.6, 161.3, 155.1, 151.9, 150.2, 149.7, 141.8, 138.3, 134.8, 130.7, 127.5, 122.1, 121.2, 117.9, 38.2, 31.8, 31.6, 26.6, 24.4, 22.3, 13.9, 11.9, 11.1; MS (FAB) *m/e* 1462 (M + 2, 100%). Anal. Calcd for $C_{80}H_{76}N_{12}O_{16}$: C, 65.74; H, 5.24; N, 11.50. Found: C, 65.57; H, 5.35; N, 11.39.

7,17:8,16-Dimetheno-9*H*,11*H*,13*H*,15*H*-quinoxalino[2″,3″:2′,3′]-[1,4]benzodioxonino[10′,9′:5,6]quinoxalino[2″,3″:2′,3′]quinoxalino-[2‴,3‴:2‴,3‴][1,4]dioxonino[6‴,5‴:9′,10′][1,4]benzodioxonino-[6′,5′:9,10][1,4]benzodioxonino[2,3-*b*]quinoxaline, 26,35,44,47-Tetramethyl-9,11,13,15-tetrapentyl-, Stereoisomer (HQx, 1). A mixture of octol **33** (1.65 g, 2 mmol), 2,3-dichloroquinoxaline (1.67 g, 8.4 mmol),

and K_2CO_3 (2.65 g) in 100 mL of DMF was stirred at 25 °C for 3 days. The product was isolated as in procedure A (silica gel–EtOAc–$CHCl_3$ (1:1, v)) to give 2.22 g (84%) of HQx (recrystallized from $CHCl_3$–hexane): ^{1}H NMR (500 MHz, $CDCl_3$, 15 mM at 20 °C) δ 7.79 (d, J = 8.1 Hz, 4 H, Ar-H), 7.64 (t, J = 8.1 Hz, 4 H, Ar-H), 7.43 (t, J = 8.1 Hz, 4 H, Ar-H), 7.15 (d, J = 8.1 Hz, 4 H, Ar-H), 6.87 (s, 2 H, Ar-H), 6.18 (s, 2 H, Ar-H), 3.52 (m, 4 H, -CH-), 3.15 (s, 6 H, Ar-CH_3), 2.24 (s, 6 H, Ar-CH_3), 1.89 (m, 4 H, -CH-CH_aH_b-), 1.77 (m, 4 H, -CH-CH_aH_b-), 1.08 (m, 24 H, -$CH_2CH_2CH_2$-CH_3), 0.68 (t, 12 H, -CH_3); dimer (500 MHz, 260 K, $CDCl_3$) δ 7.80 (d, J = 8.1 Hz, 4 H, Ar-H), 7.67 (t, J = 8.1 Hz, 4 H, Ar-H), 7.46 (t, J = 8.1 Hz, 4 H, Ar-H), 7.16 (d, J = 8.1 Hz, 4 H, Ar-H), 6.87 (s, 2 H, Ar-H), 6.17 (s, 2 H, Ar-H), 3.52 (m, 4 H, -CH-), 3.16 (s, 6 H, Ar-CH_3), 2.23 (s, 6 H, Ar-CH_3), 1.9–1.8 (m, 4 H, -CH-CH_2-), 1.06 (m, 24 H, -$CH_2CH_2CH_2$-CH_3), 0.68 (t, 12 H, -CH_3); monomer (500 MHz, 260 K, $CDCl_3$) δ 3.76 (m, -CH-), 2.52 (s, 6 H, Ar-CH_3), 2.16 (s, 6 H, Ar-CH_3), the other monomer and dimer signals overlap; MS (FAB, NOBA) m/e 1330 (M + 1, 100%). Anal. Calcd for $C_{84}H_{80}N_8O_8$: C, 75.88; H, 6.06; N, 8.43. Found: C, 75.77; H, 6.14; N, 8.25.

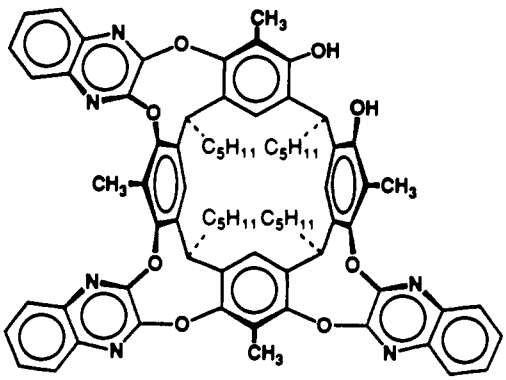

$(HO)_2$Qx, 20

9,17-Methano-11*H*),13*H*,15*H*-bisbenzo[5′,6′]quinoxalino-[2″,3″:2′,3′][1,4]benzodioxonino[10′,9′:5,6;9″,10″:8,9][1,4]dioxonino[2,3-*b*]quinoxaline-8,18-diol, 7,19,28,37-Tetramethyl-11,13,15,40-tetrapentyl-($(HO)_2$Qx, 20). A mixture of octol **33** (1.65 g, 2 mmol), 2,3-dichloroquinoxaline (1.195 g, 6 mmol), and K_2CO_3 (2 g) in 100 mL of DMF was stirred at 25 °C for 2 days. After the mixture was extracted as in procedure A, the reaction products were isolated by column chromatography (silica gel, 5% EtOAc in CH_2Cl_2 to 15% EtOAc in CH_2Cl_2). Four major fractions were separated. The most nonpolar fraction (1.82 g), which contains two components (HQx and $(HO)_2$Qx), was chromatographed again on alumina, HQx being eluted by washing the column with CH_2Cl_2; $(HO)_2$Qx was eluted with 10% CH_3OH in EtOAc; HQx, 1.1 g (41%), R_f 0.65 (silica gel, EtOAc–CH_2Cl_2 (1:9), blue fluorescence under long wave UV light); $(HO)_2$Qx, 0.73 g (30%), R_f 0.57 (silica gel, EtOAc–CH_2Cl_2 (1:9), no fluorescence under long wave UV light); mp 254–258 °C; ^{1}H NMR (500 MHz, 20 mM in $CDCl_3$ at 10 °C) δ 7.81 (d, J = 8.1 Hz, 1 H, Qx-H), 7.77 (d, J = 8.1 Hz, 1 H, Qx-H), 7.60 (m, 4 H, Qx-H), 7.43 (m, 2 H, Qx-H), 7.14 (m, 3 H, Qx-H), 6.94 (s, 2 H, Qx-H and Ar-H), 6.89 (s, 1 H, Ar-H), 6.38 (br s, 1 H, -OH), 6.23 (s, 1 H, Ar-H), 6.16 (s, 1 H, Ar-H), 4.27 (t, 1 H, -CH-), 3.49 (m, 3 H, -CH-), 3.14 (s, 3 H, Ar-CH_3), 2.73 (s, 3 H, Ar-CH_3), 2.00 (s, 3 H, Ar-CH_3), 1.52 (s, 3 H, Ar-CH_3), 1.95 (m, 4 H, -CH-CH_2-), 1.80 (m, 4 H, -CH-CH_2-), 1.15 (m, 24 H, -$CH_2CH_2CH_2$-CH_3), 0.80 (t, 3 H, -CH_3), 0.70 (m, 9 H, -CH_3); ^{1}H NMR (500 MHz, 20 mM in CD_2Cl_2 at 10 °C) δ 7.80 (d, J = 8.1 Hz, 1 H, Qx-H), 7.75 (d, J = 8.1 Hz, 1 H, Qx-H), 7.67 (m, 2 H, Qx-H), 7.57 (m, 2 H, Qx-H), 7.47 (m, 3 H, Qx-H), 7.12 (m, 3 H, Qx-H), 7.08 (br s, 1 H, -OH), 7.08 (s, 1 H, Ar-H), 6.95 (s, 1 H, Ar-H), 6.61 (br s, 1 H, -OH), 6.23 (s, 1 H, Ar-H), 6.16 (s, 1 H, Ar-H), 4.30 (t, J = 7.4 Hz, 1 H, -CH-), 3.51 (m, 1 H, -CH-), 3.43 (m, 2 H, -CH-), 3.05 (s, 3 H, Ar-CH_3), 2.68 (s, 3 H, Ar-CH_3), 1.94 (s, 3 H, Ar-CH_3), 1.45 (s, 3 H, Ar-CH_3), 2.1–1.7 (m, 8 H, -CH-CH_2-, overlap with 1.94 peak), 1.24–0.9 (m, 24 H, -$CH_2CH_2CH_2$-CH_3), 0.79 (t, 3 H, -CH_3), 0.72 (m, 9 H, -CH_3); MS (FAB, NOBA) m/e 1024 (M^+ + 2, 100%), m/e 1202 (M^+, 10%). Anal. Calcd for $C_{76}H_{78}N_5O_8$: C, 75.85; H, 6.53; N, 6.98. Found: C, 75.80; H, 6.44; N, 6.97.

9,15-(Methano[1,3]benzenomethano)-11*H*,13*H*-benzo[1″,2″:5,6;-5″,4″:5′,6′]bis[1,4]benzodioxonino[2,3-*b*:2′,3′-*b*′]diquinoxaline-8,16,33,35-tetrol, 7,17,26,34-tetramethyl-11,13,29,36-tetrapentyl-($(HO)_4$Qx syn) was isolated from the chromatograph column, 134 mg (6%), R_f 0.18 (silica gel, EtOAc–CH_2Cl_2 (1:9): ^{1}H NMR (200 MHz, $CDCl_3$) δ 7.8–7.5 (br m, 8 H, Qx-H), 6.9–6.5 (br m, 4 H, Ar-H), 4.28 (br t, 2 H, -CH-), 3.60 (br t, 2 H, -CH-), 2.6–2.0 (br m, 12 H, Ar-CH_3),

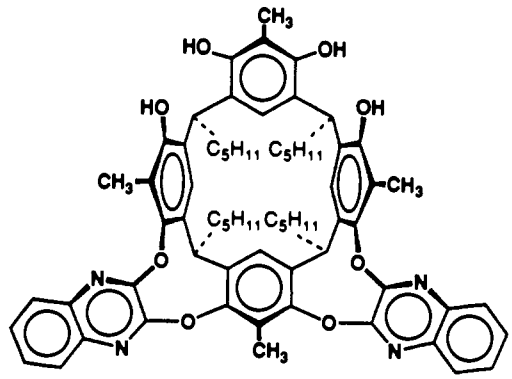

$(HO)_4$Qx *syn*

2.0 (br m, 8 H, -CH-CH_2-), 1.23 (m, 24 H, -$CH_2CH_2CH_2$-CH_3), 0.85 (m, 6 H, -CH_3), 0.75 (m, 6 H, -CH_3); MS (FAB, NOBA) m/e 1077 (M + 1, 100%).

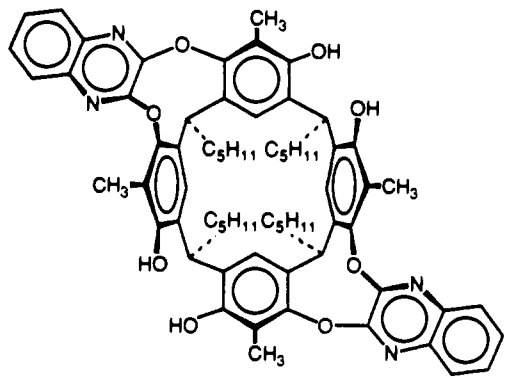

$(HO)_4$Qx *anti*

7,10:12,15:24,27:29,32-Tetraethano-8,31:14,25-dimethano-11*H*,28*H*-[1,4,14,17]tetraoxacyclohexacosino[2,3-*b*:15,16-*b*′]diquinoxaline-36,38,42,43-tetrol, 35,39,41,44-tetramethyl-11,28,37,40-tetrapentyl- ($(HO)_4$Qx anti) was isolated from the chromatograph column, 85 mg (4%), R_f 0.35 (silica gel, EtOAc–CH_2Cl_2): ^{1}H NMR (200 MHz, $CDCl_3$) δ 8.0–7.5 (br, and one sh s, 8 H, Qx-H), 6.66 (s, 2 H, Ar-H), 6.14 (s, 2 H, Ar-H), 4.26 (br t, 2 H, -CH-), 3.56 (br t, 2 H, -CH-), 2.6–2.0 (br peaks, 12 H, Ar-CH_3), 2.0–1.9 (br peaks, 8 H, -CH-CH_2-), 1.25 (m, 24 H, -$CH_2CH_2CH_2$-CH_3), 0.8 (m, 12 H, -CH_3); MS (FAB, NOBA) m/e 1077 (M + 1, 100%).

27,37:28,36-Dimetheno-29*H*,31*H*,33*H*,35*H*-dibenzo[*b*,*b*′]bis[1,7]-benzodioxonino[3,2-*j*:3′,2′-*j*′]benzo[1,2-*e*:5,4-*e*′]bis[1,3]benzodioxonin, 6,13,20,39-Tetramethyl-2,3,9,10,16,17,23,24-octanitro-29,31,33,35-tetrapentyl- ($(NO_2Bz$, 17). To a solution of octol **33** (413 mg, 0.5 mmol) and 1,2-difluoro-4,5-dinitrobenzene (**32**) (450 mg, 2.2 mmol) in 10 mL of DMA was added 670 μL of Et_3N by syringe. The clear solution was heated at 120 °C for 4 h. The product was isolated by the extraction of procedure A and then was filtered through a double-bed column which consisted of silica gel as the upper and alumina as the bottom layer, by washing with CH_2Cl_2. The slightly yellow NO_2Bz, 480 mg (65%), was obtained by evaporating solvent from the chromatogram: ^{1}H NMR (360 MHz, CD_2Cl_2) δ 7.76 (s, 4 H, H-Ar-NO_2), 7.41 (s, 4 H, H-Ar-NO_2), 7.09 (s, 2 H, Ar-H), 6.01 (s, 2 H, Ar-H), 3.91 (m, 4 H, -CH-), 2.41 (s, 6 H, Ar-CH_3), 2.16 (s, 6 H, Ar-CH_3), 2.01 (m, 8 H, -CH-CH_2-), 1.26 (m, 24 H, -$CH_2CH_2CH_2$-CH_3), 0.85 (t, J = 6.6 Hz, 12 H, -CH_3); MS (FAB, NOBA) m/e 1482 (100%, M + 2). Anal. Calcd for $C_{76}H_{72}N_8O_{24}$: C, 61.62; H, 4.90. Found: C, 61.64; H, 4.83.

27,37:28,36-Dimetheno-29*H*,31*H*,33*H*,35*H*-dibenzo[*b*,*b*′]bis[1,7]-benzodioxonino[3,2-*j*:3′,2′-*j*′]benzo[1,2-*e*:5,4-*e*′]bis[1,3]benzodioxonin, 6,13,20,39-Tetramethyl-2,3,9,10,16,17,23,24-octaamino-29,31,33,35-tetrapentyl- ($(H_2NBz$). A mixture of NO_2Bz (**17**) (1.48 g, 1 mmol) and $SnCl_2 \cdot 2H_2O$ (8.2 g, 36 mmol) was suspended in 150 mL of anhydrous EtOH under argon. It was heated at 100 °C for 1 h to suspend the solid. Then 30 mL of concentrated hydrochloric acid was added slowly. Upon reduction, the yellow mixture turned to a white emulsion. Heating was continued at 100 °C for 5 h. The solvent was removed in vacuo, and the white residue was redissolved in water and then made basic with strong aqueous KOH. The product was extracted with CH_2Cl_2, and the CH_2Cl_2 layer was dried ($MgSO_4$) and concentrated in vacuo. The crude residue

was chromatographed on silica gel–10% MeOH in CH_2Cl_2. The product was eluted with 100% MeOH. The slightly brown-colored solid of H_2NBz, 820 mg (66%) was obtained by evaporating the filtrate to dryness under high vacuum: ^1H NMR (360 MHz, CD_2Cl_2) δ 6.91 (s, 2 H, Ar-H), 6.55 (s, 4 H, H-Ar-NH_2), 6.12 (s, 4 H, H-Ar-NH_2), 5.87 (s, 2 H, Ar-H), 4.22 (br t, 4 H, -CH-), 2.34 (s, 6 H, Ar-CH_3), 2.06 (s, 6 H, Ar-CH_3), 1.89 (m, 8 H, -CH-CH_2-), 1.24 (m, 24 H, -$CH_2CH_2CH_2$-CH_3), 0.83 (t, J = 6.5 Hz, 12 H, -CH_3).

27,37:28,36-Dimetheno-29*H*,31*H*,33*H*,35*H*-dibenzo[*b*,*b*']bis[1,7]benzodioxonino[3,2-*j*:3',2'-*j*']benzo[1,2-*e*:5,4-*e*']bis[1,3]benzodioxonin, 6,13,20,39-Tetramethyl-2,3,9,10,16,17,23,24-octakis(*p*-toluenesulfonamido)-29,31,33,35-tetrapentyl- (HNTsBz). A mixture of H_2NBz (807 mg, 0.65 mmol) and *p*-$MeC_6H_4SO_2Cl$ (1.288 g, 6.7 mmol) in 20 mL of pyridine was stirred at 25 °C for 16 h. The solvent was evaporated in vacuo, and the residue was partitioned between CH_2Cl_2 and water. The CH_2Cl_2 layer was concentrated. The residue was suspended in MeOH and boiled to dissolve impurities. The solid was filtered, washed (MeOH), and dried under high vacuum to give 1.21 g (75%) of HNTsBz: ^1H NMR (360 MHz, $CDCl_3$) δ 8.60 (br s, 8 H, -NH-), 7.6 (d, 8 H, tosyl-ArH), 7.33 (m, 8 H, tosyl-ArH), 7.18 (d, 8 H, tosyl-ArH), 7.10 (d, 8 H, tosyl-ArH), 6.84 (s, 2 H, Ar-H), 6.82 (s, 4 H, TsN-Ar-H), 6.24 (s, 4 H, TsN-Ar-H), 5.71 (s, 2 H, Ar-H), 3.65 (t, 4 H, -CH-), 2.32 (s, 12 H, CH_3-tosyl), 2.19 (s, 18 H, CH_3-tosyl and Ar-CH_3), 2.26 (s, 6 H, Ar-CH_3), 1.83 (br m, 8 H, -CH-CH_2-), 1.4–1.1 (m, 24 H, -$CH_2CH_2CH_2$-CH_3), 0.83 (t, J = 6.75 Hz, 12 H, -CH_3).

27,37:28,36-Dimetheno-29*H*,31*H*,33*H*,35*H*-dibenzo[*b*,*b*']bis[1,7]benzodioxonino[3,2-*j*:3',2'-*j*']benzo[1,2-*e*:5,4-*e*']bis[1,3]-benzodioxonin, 6,13,20,39-Tetramethyl-2,3,9,10,16,17,23,24-octakis(*N*-methyl-*p*-toluenesulfonamido)-29,31,33,35-tetrapentyl- (MeNTsBz). To a mixture of HNTsBz (1.21 g, 0.488 mmol) and K_2CO_3 (1.08 g) in 50 mL of DMF was added 1 mL of CH_3I by syringe. The mixture was stirred at 25 °C for 16 h. The solvent was removed in vacuo. The residue was partitioned between CH_2Cl_2 and water, and the CH_2Cl_2 layer was dried ($MgSO_4$) and concentrated. The residue was chromatographed on a silica gel column which was washed with CH_2Cl_2 to remove nonpolar impurities. The product was eluted by washing with EtOAc–hexane (1:1, v) to give 1.20 g (95%) of MeNTsBz. The slightly yellow solid was obtained after removing solvent from the eluent: ^1H NMR (360 MHz, $CDCl_3$) δ 7.81 (d, J = 7.8 Hz, 8 H, tosyl-ArH), 7.72 (d, J = 7.8 Hz, 8 H, tosyl-ArH), 7.37 (t (d of d), 16 H, tosyl-ArH), 7.00 (s, 2 H, Ar-H), 6.64 (br s, 4 H, MeN-Ar-H), 6.30 (br s, 4 H, MeN-Ar-H), 5.89 (s, 2 H, Ar-H), 3.99 (m, 4 H, -CH-), 3.18 (s, 12 H, -NCH_3), 3.02 (s, 12 H, -NCH_3), 2.48 (s, 12 H, tosyl-CH_3), 2.41 (s, 12 H, tosyl-CH_3), 2.30 (s, 6 H, Ar-CH_3), 2.05 (s, 6 H, Ar-CH_3), 2.06 (br m, 4 H, -CH-CH_aH_b-), 1.90 (br m, 4 H, -CH-CH_aH_b-), 1.28 (m, 24 H, -$CH_2CH_2CH_2$-CH_3), 0.89 (t, 12 H, -CH_3).

27,37:28,36-Dimetheno-29*H*,31*H*,33*H*,35*H*-dibenzo[*b*,*b*']bis[1,7]benzodioxonino[3,2-*j*:3',2'-*j*']benzo[1,2-*e*:5,4-*e*']bis[1,3]benzodioxonin, 6,13,20,39-Tetramethyl-2,3,9,10,16,17,23,24-octakis(N-methylamino)-29,31,33,35-tetrapentyl- (HNMeBz). A 0.1 M solution of sodium anthracenide in THF was prepared by dissolving 2 g (11.2 mmol) of anthracene (recrystallized from EtOH) and 250 mg (5 mmol) of Na in 100 mL of dry THF under argon. After stirring for 2 h, dissolution was complete, and a dark blue color persisted. To a solution of MeNTsBz (600 mg, 0.23 mmol) in 100 mL of THF at 0 °C was added 80 mL of anthracenide solution (8 mmol) by a double-tipped needle. The mixture was stirred for 4 min and quenched by adding 5 mL of brine. The solvent was removed in vacuo, and the residue was extracted with CH_2Cl_2 and water. The organic layer was dried ($MgSO_4$) and concentrated to a volume of 50 mL. This solution was filtered through a silica gel column by washing with CH_2Cl_2 to remove anthracene. The product was eluted by washing with MeOH. The solid obtained by evaporating the filtrate was further purified by filtering through alumina–EtOAc–hexane (1:1, v)–MeOH mixtures to give 220 mg (70%) of HNMeBz as a slightly brown solid: ^1H NMR (360 MHz, $CDCl_3$) δ 6.92 (s, 2 H, Ar-H), 6.50 (s, 4 H, MeN-Ar-H), 6.09 (s, 4 H, MeN-Ar-H), 5.91 (s, 2 H, Ar-H), 4.24 (m, 4 H, -CH-), 3.5–2.5 (br 4 H, -NH-), 3.25 (q, J = 5.3 Hz, 4 H, -NH-), 2.86 (d, J = 5.3 Hz, 12 H, -N-CH_3), 2.61 (d, J = 5.3 Hz, 12 H, -N-CH_3), 2.41 (s, 6 H, Ar-CH_3), 2.19 (s, 6 H, Ar-CH_3), 1.92 (br m, -CH-), 1.30 (m, 24 H, -$CH_2CH_2CH_2$-CH_3), 0.85 (t, 12 H, -CH_3); ^{13}C NMR (90 MHz, $CDCl_3$) δ 153.1, 151.5, 142.2, 136.2, 136.0, 133.8, 132.4, 130.7, 123.2, 122.3, 118.2, 117.4, 105.6, 101.0, 40.9, 35.8, 32.0, 31.8, 31.2, 30.7, 26.7, 22.5, 14.1, 10.9.

6,16:7,15-Dimetheno-2*H*,8*H*,10*H*,12*H*,14*H*,20*H*,28*H*,36*H*-benzimidazo[5'',6'':2',3'][1,4]benzodioxonino[10',9':5,6]benzimidazo[5'',6'':2',3']benzimidazo[5'''',6'''':2''',3''']-[1,4]dioxonino[6''',5''':9',10']-[1,4]benzodioxonino[6',5':9,10][1,4]benzodioxonino[2,3-*f*]benzimidazole-2,20,28,36-tetrone, 1,3,19,21,27,29,35,37-Octahydro-1,3,19,21,24,27,29,32,35,37,40,43-dodecamethyl-8,10,12,14-tetrapentyl- (UreaBz, 18). To a solution of HNMeBz (68 mg, 0.05 mmol) and triphosgene (60 mg, 0.2 mmol) in 20 mL of THF under argon at 25 °C was added 50 μL of Et_3N. The solution was stirred at 25 °C for 5 h. The product was isolated as in procedure A after chromatography on silica gel–10% MeOH in CH_2Cl_2 to give 25 mg (34%) of UreaBz as a solid: ^1H NMR (500 MHz, $CDCl_3$) δ 6.89 (s, 2 H, Ar-H), 6.48 (s, 4 H, MeN-Ar-H), 6.09 (s, 4 H, MeN-Ar-H), 5.99 (s, 2 H, Ar-H), 4.17 (m, 4 H, -CH-), 3.40 (s, 12 H, -N-CH_3), 3.29 (s, 12 H, -N-CH_3), 2.69 (s, 6 H, Ar-CH_3), 1.85 (s, 6 H, Ar-CH_3), 1.9 (br m, 4 H, -CH_aH_b-), 1.80 (br m, 4 H, -CH_aH_b-), 1.15 (m, 24 H, -$CH_2CH_2CH_2$-CH_3), 0.77 (t, 12 H, -CH_3); ^{13}C NMR (90 MHz, $CDCl_3$) δ 154.5, 152.8, 150.9, 143.9, 139.1, 134.3, 129.0, 126.2, 124.9, 123.8, 122.4, 117.8, 115.4, 100.9, 96.6, 35.3, 31.8, 31.6, 27.5, 26.9, 26.6, 22.4, 14.1, 12.6, 10.9; MS (FABS, NOBA) m/e 1457 (M^+ + 1, 100%). Anal. Calcd for $C_{88}H_{96}N_8O_{12}$: C, 72.51; H, 6.64. Found: C, 72.24; H, 6.73.

Systematic Names, Syntheses, and Full Characterizations Relegated to the Supplementary Material. Complete data are found for the following compounds: MeOPz, **9**; MeSPz, **10**; Me_2NPz, **11**; FMeNPz, **19** (plus structural formula); EtPz, **7**; CNPz, **12**; MeQx, **13**; ClQx, **14**; and BrQx, **15**.

Crystal Structure Determinations. Complete HQx·HQx·3$(CH_3)_2CO$ (**1**·**1**·3$(CH_3)_2CO$) crystallizes from CH_3COCH_3 as colorless parallelepipeds in the monoclinic system $C2/c$. Cell dimensions are as follows: a = 23.780 (2) Å, b = 31.251 (3) Å, c = 23.391 (1) Å, β = 93.900 (4)°, V = 16 308 Å^3, Z = 4 (there are four dimers or eight monomeric units in the cell). The crystal was examined on a modified Huber diffractometer, Mo Kα radiation, at 295 K. The structure was determined by direct methods. Refinement of two blocks of parameters (213 + 218), 10 662 unique reflections, and 2975 reflections with $I > 3\sigma(I)$) has an agreement value, R, currently at 0.17. The solvent is disordered.

Compound **2** crystallizes from $C_6H_5NO_2/CH_2Cl_2/CHCl_3/CH_3COOC_2H_5$ as colorless parallelepipeds in the monoclinic system $C2/c$. Cell dimensions are as follows: a = 38.71 (1) Å, b = 8.907 (8) Å, c = 30.260 (8) Å, β = 114.53 (1)°, V = 9493 Å^3, Z = 4 (the monomer has a 2-fold axis). The crystal was examined on a modified Syntex P$\bar{1}$ diffractometer, Cu Kα radiation, at 295 K. The structure was determined by direct methods. Refinement of 261 parameters, 4878 unique reflections, and 1437 reflections with $I > 3\sigma(I)$) has an agreement value, R, currently at 0.17. The solvent is disordered. The methyl carbon of one of the two unique ethyl groups is disordered. The monomer packs "head to tail".

Complex ClPz·ClPz·8$C_6H_5NO_2$ (**4**·**4**·$C_6H_5NO_2$) crystallizes from $C_6H_5NO_2$ as colorless plates in the triclinic system P$\bar{1}$. Cell dimensions are as follows: a = 19.1995 (8) Å, b = 20.7840 (9) Å, c = 26.130 (1) Å, α = 89.235 (2), β = 85.690 (1), γ = 66.966 (1)°, V = 9567 Å^3, Z = 2 (there are two dimers or four monomeric units in the cell). The crystal was examined on a modified Syntex P$\bar{1}$ diffractometer, Cu Kα radiation, at 295 K. The structure was determined by direct methods. Refinement of three blocks of parameters (433 + 433 + 197), 19 570 unique reflections, 6575 reflections with $I > 3\sigma(I)$) has an agreement value, R, currently at 0.12. Some of the solvent is disordered.

Complex HPz·HPz·$n$$C_6H_5CH_3$ (**5**·**5**·$n$$C_6H_5CH_3$) crystallizes from $CH_3C_6H_5$ as colorless crystalline plates in the triclinic system P$\bar{1}$. Unit cell dimensions are as follows: a = 19.864 (1) Å, b = 20.789 (1) Å, c = 21.244 (1) Å, α = 86.649 (1), β = 69.100 (1), γ = 82.367 (1)°, V = 8122 Å^3, Z = 2 (two dimers or four monomeric units in the cell). The crystal was examined on a modified Syntex P$\bar{1}$ diffractometer, Cu Kα radiation, at 295 K. The structure was determined by direct methods. Refinement of three blocks (337 + 321 + 113 parameters), 16691 unique reflections, and 5825 reflections with $I > 3\sigma(I)$ has an agreement value, R, currently at 0.22. There are possibly nine uncharacterized solvent molecules per dimer. None of these is easily recognized as toluene.

Complex $CH_3Pz·CH_3Pz·7C_6H_5NO_2$ (6·6·7$C_6H_5NO_2$) crystallizes from $C_6H_5NO_2$ as colorless parallelepipeds in the triclinic system P$\bar{1}$. Cell dimensions are as follows: a = 19.122 (1) Å, b = 19.944 (1) Å, c = 32.084 (2) Å, α = 96.289 (1), β = 97.531 (2), γ = 107.961 (1)°, V = 11393 Å^3, Z = 2 (there are two dimers or four monomeric units in the cell). The crystal was examined on a modified Syntex P$\bar{1}$ diffractometer, Cu Kα radiation, at 295 K. The structure was determined by direct methods. Refinement of three blocks of parameters (393 + 369 + 137), 23 385 unique reflections, and 7616 reflections with $I > 3\sigma(I)$) has an agreement value, R, currently at 0.25. Approximately $^1/_3$ of the crystal contents is solvent. At least 14 $C_6H_5NO_2$ molecules are present in the unit cell, and other uncharacterized solvent molecules appear on a difference electron density map.

Complex FMeNPz·FMeNPz·2(solvent) (**19**·**19**·2(solvent)) crystallizes from CH_2Cl_2/CH_3NO_2 as yellow parallelepipeds in the tetragonal system $I4_1/a$. Unit cell dimensions are as follows: a = 29.011 (3) Å, c = 21.224 (2) Å, V = 17862 Å^3, Z = 4 (four dimers in the unit cell or $^1/_4$ dimer in the asymmetric unit). A 2-fold axis passes through each monomer and two monomers are related by a $\bar{4}$ axis. The crystal was examined on a modified Syntex P$\bar{1}$ diffractometer, Cu Kα radiation, at 295 K. The

structure was determined by direct methods. Refinement of two blocks (190 + 32 parameters), 4217 unique reflections, and 1923 reflections with $I > 1.5\sigma(I)$ has an agreement value, R, currently at 0.23. Two unidentified solvent molecules seem to be present in each asymmetric unit (32 in the unit cell).

Equilibrium Constant Measurements. NMR solvents used in equilibrium constant measurement were purchased from Aldrich as the highest atom % deuterated compounds in a glass vial, i.e., $(CD_3)_2CO$, 100.0% atom D; CD_3CN, 100.0% atom D; C_6D_6, 100.0% atom D; ClC_6D_5, 98.5% atom D; $(CD_2)_6$, 99.5% atom D; $(CD_3)_2NCDO$, 99.5% atom D; C_2D_5OD, anhydrous, 99+% atom D; $(CD_2)_4O$, 99.5% atom D; $CD_3C_6D_5$, 100.0% atom D; $CDCl_3$, 100.0% atom D; CD_2Cl_2, 100.0% atom D and CCl_4, which was distilled from P_2O_5, and were opened under argon prior to preparing NMR samples.

Samples were weighed on a microbalance, Mettler Instrument (1 div = 0.1 mg). The sample was dissolved in 0.5 mL or 1.0 mL of deuterated solvent in a 5-mm NMR tube. Relatively concentrated NMR samples higher than 1.0 mM concentration were prepared by weighing solid samples, transferring into a NMR tube, drying the NMR tube in a pistol under high vacuum at 60 °C overnight, filling the pistol with argon, followed by adding the NMR solvent to the NMR tube under argon by syringe. The NMR sample was stored in a refrigerator. The dilute samples (concentration <1.0 mM stock solution) were prepared from a 1.0 mM stock solution. Specific amounts of 1.0 mM stock solution were transferred into a NMR tube by a microsyringe. The sample in the tube was concentrated to dryness by flowing argon gas into the tube. The NMR tube was then dried in a pistol, and the procedures were followed as described above.

The ^1H NMR spectra were recorded on a Bruker AM 500 at 500 MHz. The temperature was measured at desired points on the scale by using a MeOH-temperature calibrating sample. For comparison of data at specific temperatures, generally 30 °C to -50 °C, temperatures over 5 or 10 °C intervals were used. The temperature was calculated from observed chemical shift difference due to CH_3 and OH resonances by using the following equation:[24]

$$T(K) = 403 - \frac{29.5}{M}\Delta\nu - \frac{23.81}{M^2}(\Delta\nu)^2$$

where M is the spectrometer frequency (Hz) and $\Delta\nu$ is the chemical shift difference between CH_3 and OH resonances (Hz). The peaks employed were integrated with ±10% error.

Supplementary Material Available: Table I, association constants for homodimerization in $CDCl_3$, and Table II, association constants for heterodimerization in $CDCl_3$, section on known bridging compounds, systematic names, syntheses, and full characterizations of **7** and **9-15**, and structure of FMeNPz **19** (15 pages). Ordering information is given on any current masthead page.

Constrictive and Intrinsic Binding in a Hemicarcerand Containing Four Portals[1,2]

Donald J. Cram,* Michael T. Blanda, Kyungsoo Paek, and Carolyn B. Knobler

Contribution from the Department of Chemistry and Biochemistry, University of California at Los Angeles, Los Angeles, California 92004. *Received April 1, 1992*

Abstract: The synthesis, crystal structure, and binding properties are reported for a globe-shaped hemicarcerand (**4**) composed of two rigid bowl-like units (polar caps) attached to one another at their rims through four *o*-xylyl units (equatorial spacers). Four pendant β-phenylethyl groups attached to each of the polar caps impart solubility to the system. The critical shell-closing reaction, $2Ar(OH)_4 + 4\,o\text{-}C_6H_4(CH_2Br)_2$ (+ base) → $Ar(OCH_2C_6H_4CH_2O)_4Ar$, went in 20-25% yields in $(CH_3)_2NCOCH_3$ as solvent, one molecule of which is a template for the eight bond-forming reactions and becomes a guest in the hemicarceplex, stable at 25 °C. In the crystal structure of the complex, the guest is disordered, and one polar cap is rotated 21° about the polar axis with respect to the other polar cap. This rotation minimizes the internal volume and surface area of the system and closes the portals. When heated at 100 °C in a series of solvents whose volumes and shapes are complementary to those of the inner phase of **4**, complex **4**·$(CH_3)_2NCOCH_3$ underwent guest exchange with solvent to give **4**·solvent at 100-120 °C; the exchange rate decreased in the following sequence of solvents used: $C_6D_5Br \geq C_6D_5Cl > 1,2\text{-}(CD_3)_2C_6D_4 > C_6D_5CD_3 > 1,4\text{-}CD_3C_6D_4CD_3 > Cl_2CDCDCl_2$. Empty host **4** in differing maximum amounts was detected as an intermediate in these guest substitution reactions. First-order rates for guest loss to solvent in $CDCl_2CDCl_2$ at 100 °C decreased with guest change as follows: $CH_3CN > (CH_3)_2NCOCH_3 \approx (CH_3)_2NCHO > C_6H_5CH_3 \approx MeCOEt > BuOH > CHCl_2CHCl_2 > EtOAc$. Solvents too large to enter **4** were *o*-$(CH_3)_2C_6H_4$, *m*-$(CH_3)_2C_6H_4$, *p*-$CH_3C_6H_4CH_2CH_3$, *p*-$(CH_3CH_2)_2C_6H_4$, *p*-$CH_3C_6H_4CH(CH_3)_2$, $(CH_3)_3CC_6H_5$, 1,3,5-$(CH_3)_3C_6H_3$, and *p*-$(CH_3)_2CHC_6H_4CH(CH_3)_2$. Heating **4**·$(CH_3)_2NCOCH_3$ in *p*-$(CH_3)_2CHC_6H_4CH(CH_3)_2$ to 160 °C for 24 h produced empty **4**, which in 1,2-$(CD_3)_2C_6D_4$ at temperatures ranging from 80 to 130 °C was submitted to in and out rate measurements (^1H NMR) with $(CH_3)_2NCOCH_3$, $CH_3CH_2O_2CCH_3$, $CH_3CH_2COCH_3$, and $C_6H_5CH_3$ as guests. Association constants, $\Delta G°$, ΔH, ΔS, $\Delta G^{\ddagger}_{in}$, and $\Delta G^{\ddagger}_{out}$ were calculated and are discussed in terms of intrinsic and constrictive free energy contributions to the activation free energies for dissociation. With $CH_3CH_2O_2CCH_3$, $(CH_3)_2NCOCH_3$, and $CH_3CH_2COCH_3$, the associations were both enthalpy and entropy driven to provide $-\Delta G°$ values at 100 °C of 3.8, 3.7, and 5.3 kcal mol^{-1}, respectively. With $C_6H_5CH_3$, the complexation was entropy driven, but enthalpy opposed to give a $-\Delta G°$ value (100 °C) of 3.4 kcal mol^{-1}. These effects are interpreted in terms of the relative rigidities of the guests, the liberation of complexing solvent upon incarceration, the conversion of *inner consolidated* into *dispersed outer space* of the host upon complexation, and host-guest attractive forces between complexing partners.

In prior papers of this series, we reported the syntheses and binding properties of two types of hemicarcerands. The first type[3,4] was composed of two polar caps possessing C_4 axes attached to one another with three short spacer units [$(OCH_2O)_3$], leaving a fourth possible position as a portal for entry or egress of potential guests (**1**). The inner space of this host proved to have unique properties of constraining or enhancing (depending on spacial relationships) conformational reorganizations of guests, of providing a nonsolvating environment for carrying out chemical reactions,[3,4] and as a phase in which cyclobutadiene could be synthesized and preserved at room temperature.[5] The second type of hemicarcerand (**2**) made use of the same polar caps coupled

(1) Host-Guest Complexation. 63.

(2) We warmly thank the U.S. Public Health Services for supporting Grant GM-12640 and the National Science Foundation for supporting Grant NSF CHE 8802800.

(3) Tanner, M. E.; Knobler, C. B.; Cram, D. J. *J. Am. Chem. Soc.* **1990**, *112*, 1659-1660.

(4) Cram, D. J.; Tanner, M. E.; Knobler, C. B. *J. Am. Chem. Soc.* **1991**, *113*, 7717-7727.

(5) Cram, D. J.; Tanner, M. E.; Thomas, R. *Angew. Chem., Int. Ed. Engl.* **1991**, *30*, 1024-1027.

0002-7863/92/1514-7765$03.00/0